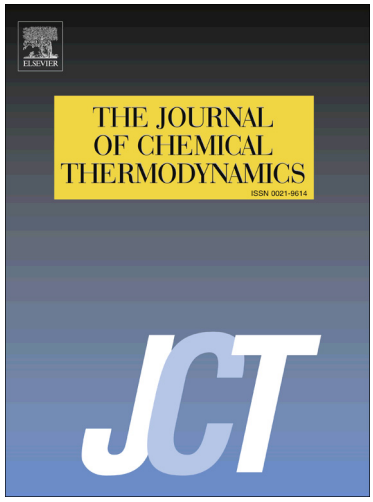

Thermodynamics of amide + amine mixtures. 4. Relative permittivities of *N,N*-dimethylacetamide + *N*-propylpropan-1-amine, + *N*-butylbutan-1-amine, + butan-1-amine, or + hexan-1-amine systems and of *N,N*-dimethylformamide + aniline mixture at several temperatures. Characterization of amine + amide systems using ERAS

Fernando Hevia, Juan Antonio González, Ana Cobos, Isaías García de la Fuente, Luis Felipe Sanz

PII: S0021-9614(17)30408-1
DOI: https://doi.org/10.1016/j.jct.2017.11.011
Reference: YJCHT 5262

To appear in: *J. Chem. Thermodynamics*

Received Date: 2 June 2017
Revised Date: 6 November 2017
Accepted Date: 20 November 2017

Please cite this article as: F. Hevia, J.A. González, A. Cobos, I. García de la Fuente, L.F. Sanz, Thermodynamics of amide + amine mixtures. 4. Relative permittivities of *N,N*-dimethylacetamide + *N*-propylpropan-1-amine, + *N*-butylbutan-1-amine, + butan-1-amine, or + hexan-1-amine systems and of *N,N*-dimethylformamide + aniline mixture at several temperatures. Characterization of amine + amide systems using ERAS, *J. Chem. Thermodynamics* (2017), doi: https://doi.org/10.1016/j.jct.2017.11.011

Thermodynamics of amide + amine mixtures. 4. Relative permittivities of *N*,*N*-dimethylacetamide + *N*-propylpropan-1-amine, + *N*-butylbutan-1-amine, + butan-1-amine, or + hexan-1-amine systems and of *N*,*N*-dimethylformamide + aniline mixture at several temperatures. Characterization of amine + amide systems using ERAS

Fernando Hevia, Juan Antonio González*, Ana Cobos, Isaías García de la Fuente, Luis Felipe Sanz

G.E.T.E.F., Departamento de Física Aplicada, Facultad de Ciencias, Universidad de Valladolid, Paseo de Belén, 7, 47011 Valladolid, Spain.

*e-mail: jagl@termo.uva.es; Fax: +34-983-423136; Tel: +34-983-423757

Abstract

Relative permittivities at 1 MHz, ε_r, and at (293.15-303.15) K are reported for the binary systems *N,N*-dimethylacetamide (DMA) + *N*-propylpropan-1-amine (DPA), + *N*-butylbutan-1-amine (DBA), + butan-1-amine (BA) or + hexan-1-amine (HxA) and for *N,N*-dimethylformamide (DMF) + aniline. The excess permittivities, ε_r^E, are large and negative for systems with DMA, whereas they are large and positive for the aniline mixture. From the analysis of these ε_r^E data and of measurements previously reported, it is concluded: (i) the main contribution to ε_r^E in systems with linear amines arises from the breaking of interactions between like molecules; (ii) in the DMF + aniline mixture, interactions between unlike molecules contribute positively to ε_r^E, and such a contribution is dominant; (iii) longer linear amines are better breakers of the amide-amide interactions; (iv) interactions between unlike molecules are more easily formed when shorter linear amines, or DMF, participate. These findings are confirmed by a general study conducted in terms of excess values of molar orientational and induced polarizabilities and of the relative Kirkwood correlation factors for systems and components. The ERAS model is also applied to amide + amine mixtures. ERAS represents rather accurately the excess enthalpies and volumes of the mentioned systems. The variation of the cross-association equilibrium constants, determined using ERAS, with the molecular structure is in agreement with that observed for ε_r^E.

Keywords: Amides; amines; permittivity, Kirkwood correlation factor; excess functions; ERAS.

1. Introduction

The chemical environment of proteins is highly complex. A suitable approach for its investigation is to focus on small organic molecules which are more or less similar to the functional groups which constitute the biomolecule [1]. In this framework, the determination of thermodynamic, transport and dielectric properties for the mentioned molecules and for their mixtures is necessary, as information on interactions in condensed phase environments can be inferred from these properties.

Amides are a very important class of organic solvents due to their high polarity (the dipole moment of *N,N*-dimethylformamide (DMF) and *N,N*-dimethylacetamide (DMA) is 3.7 D [2,3]), strong solvating power and liquid state range [4]. The latter is strongly linked to the ability of amides to form hydrogen bonds. It is well known that primary and secondary amides are self-associated species, while tertiary amides show a relevant local order due to the existence of strong dipolar interactions between their molecules [5,6]. This makes amides useful as model systems for peptides [6].

The amine group is also encountered in substances of great biological interest. For example, histamine and dopamine act as neurotransmitters [7,8], and the breaking of amino acids releases amines. On the other hand the proteins usually bound to DNA polymers contain various amine groups [9]. Interestingly, primary and secondary amines are self-associated compounds [10-14] with low dipole moments in the case of linear amines (1.3 D for BA and 1.0 D for DPA [15]). The dipole moment of aniline (1.51 D [3]) is higher and proximity effects between the phenyl ring and the amine group lead to strong dipolar interactions between aniline molecules. As a consequence, aniline + *n*-alkane mixtures are characterized by relatively high upper critical solution temperatures (343.1 K for the heptane solution [16]).

The study of amine + amide systems is then relevant as it allows to gain insight into the amide group behaviour when it is surrounded by different environments. In fact, the hydrogen-bonded structures where the amide group is involved can show very different biological activities depending on the mentioned environments [17].

The few data available in the literature on excess molar enthalpies, H_m^E, for amine + amide mixtures underline the importance of interactions between unlike molecules in such systems. For example, at equimolar composition, we have H_m^E/J·mol^{-1} = −2946 (aniline + DMF, T = 298.15 K) [18]; −352 (aniline + DMA, T = 298.15 K) [19], −1000 (HxA + *N*-methylacetamide (NMA), T = 363.15 K) [20]. Interestingly, H_m^E/J·mol^{-1} values of methanol + NMA (−76, T = 313.15 K) [21], or + DMA (−737; T = 298.15 K) [22] are very different.

In previous studies, we have reported data on density, ρ, speed of sound, c, and refractive index, n_D, for the binary systems DMF [23], or DMA [24] + *N*-propylpropan-1-amine (DPA) or + butan-1-amine (BA) at (293.15-303.15) K, and + *N*-butylbutan-1-amine (DBA) or + hexan-1-amine (HxA) at 298.15 K. These data have interpreted in terms of solute-solvent interactions and structural effects [23,24]. On the other hand, we have also reported permittivity measurements for the DMF + BA, + HxA, + DPA, + DBA systems at (293.15-303.15) K [25]. As a continuation of these works, we provide now low-frequency relative permittivities, ε_r, for the DMA + BA, + HxA, + DPA, + DBA mixtures, and for the DMF + aniline system at the same temperature range. The replacement of DMF by DMA in the mentioned systems including linear amines may be useful to investigate steric/size effects on the excess ε_r values. The aniline + DMF system has been selected on the basis of its very large and negative H_m^E value. The present study is completed by the application of different theories. Firstly, amine + amide mixtures are studied using the ERAS model [26]. Secondly, the ε_r data reported here are used together with the corresponding ρ and n_D values available in the literature [23,24,27] to determine orientational and induced polarizabilities according to the Kirkwood-Fröhlich model [28-31] and the Balankina relative excess Kirkwood correlation factors [32], very useful quantities to gain insight into the dipole correlations present in the mixtures under consideration.

2. Experimental

2.1 Materials

Table 1 collects information regarding the source and purity of the pure compounds, which have been used with no further purification.

2.2 Apparatus and procedure

Binary mixtures were prepared by mass in small vessels of about 10 cm^3, using an analytical balance Sartorius MSU125p (weighing accuracy 0.01 mg), with all weighings corrected for buoyancy effects. The standard uncertainty in the final mole fraction is estimated to be 0.0010. Molar quantities were calculated using the relative atomic mass Table of 2015 issued by the Commission on Isotopic Abundances and Atomic Weights (IUPAC) [33]. In order to minimize the effects of the interaction of amines with air components, they were stored with 4 Å molecular sieves; also, the measurement cell (see below) was completely filled with the samples and appropriately closed. Different density measurements of pure compounds, conducted along experiments, showed that this quantity remained unchanged within the experimental uncertainty.

Temperatures were measured by means of Pt-100 resistances, calibrated according to the ITS-90 scale of temperature, against two fixed points: the triple point of the water and the fusion point of Ga. The standard uncertainty of the equilibrium temperature measurements is 0.01 K and the corresponding accuracy is 0.02 K.

Permittivity measurements were conducted using a 16452A cell (parallel-plate capacitor) connected, by means of a 16048G test lead, to a precision impedance analyser 4294A; all of them are from Agilent. The 16452A cell is made of Nickel-plated cobalt (54% Fe, 17% Co, 29% Ni) with a ceramic insulator (alumina, Al_2O_3). The volume of the sample filling the cell is ≈ 4.8 cm^3. The temperature was controlled by a thermostatic bath LAUDA RE304, (temperature stability: 0.02 K). Details about the device configuration and calibration can be found elsewhere [34]. The relative standard uncertainty of the ε_r measurements (i.e. the repeatability) is 0.0001. The total relative standard uncertainty of ε_r was estimated to be 0.003 from the differences between our data and values available in the literature for the following pure liquids in the temperature range (288.15–333.15) K: water, benzene, cyclohexane, hexane, nonane, decane, dimethyl carbonate, diethyl carbonate, methanol, 1-propanol, 1-pentanol, 1-hexanol, 1-heptanol, 1-octanol, 1-nonanol and 1-decanol.

Our experimental ε_r values, at 1 MHz and 0.1 MPa, of pure compounds, together with literature data, are shown in Table 2. We note the excellent agreement encountered between them for DMF and DMA. Larger discrepancies between such data are observed for amines, which may be ascribed to the different source and purity of the amines used in the literature. In fact, inspection of Table 2 shows that, for example, some ε_r values of aniline taken from the literature are not sure as they do not change consistently with temperature. In contrast, our ε_r values correctly decrease with the increasing of temperature, and the density measurements are in good agreement with literature data (Table S1, supplementary material; see also [23,24] for the remaining amines).

3. Experimental results

The relative permittivity of an ideal mixture at the same temperature and pressure as the solution under study, ε_r^{id}, is calculated from the expression [35]:

$$\varepsilon_r^{id} = \phi_1 \varepsilon_{r1}^* + \phi_2 \varepsilon_{r2}^* \qquad (1)$$

where the volume fraction of component i is defined as $\phi_i = x_i V_{mi}^* / V_m^{id}$; x_i represents the mole fraction of component i, V_{mi}^* and ε_{ri}^* stand for the molar volume and relative permittivity of

pure component i respectively, and $V_{\mathrm{m}}^{\mathrm{id}} = x_1 V_{\mathrm{m1}}^{*} + x_2 V_{\mathrm{m2}}^{*}$ is the ideal molar volume of the mixture at the same temperature and pressure. The excess relative permittivity, $\varepsilon_{\mathrm{r}}^{\mathrm{E}}$, is obtained as

$$\varepsilon_{\mathrm{r}}^{\mathrm{E}} = \varepsilon_{\mathrm{r}} - \varepsilon_{\mathrm{r}}^{\mathrm{id}} \qquad (2)$$

where ε_r is the permittivity of the mixture. The necessary volumetric properties were obtained from the literature [23,24,27] (see also footnote of Table 2). Table 3 lists ϕ_1, ε_r and $\varepsilon_{\mathrm{r}}^{\mathrm{E}}$ values for DMA (1) + amine (2), or DMF (1) + aniline (2) systems as functions of the mole fraction of the amide, x_1, in the temperature range (293.15 – 303.15) K. Results are shown graphically in Figures 1-3 (see also Figure S1, supplementary material). The only data available in the literature [36] for comparison are those for the DMF + aniline system at 303.15 K. They largely differ from our measurements (Figure S2, supplementary material).

The $\varepsilon_{\mathrm{r}}^{\mathrm{E}}$ data have been fitted by an unweighted linear least-squares regression to a Redlich-Kister equation:

$$\varepsilon_{\mathrm{r}}^{\mathrm{E}} = x_1 (1 - x_1) \sum_{i=0}^{k-1} A_i (2x_1 - 1)^i \qquad (3)$$

For each system, the number, k, of necessary coefficients for this regression has been determined by applying an F-test of additional term [37] at 99.5% confidence level. Table 4 includes the parameters A_i obtained, and the standard deviations $\sigma(\varepsilon_{\mathrm{r}}^{\mathrm{E}})$, defined by:

$$\sigma(\varepsilon_{\mathrm{r}}^{\mathrm{E}}) = \left[\frac{1}{N-k} \sum_{j=1}^{N} \left(\varepsilon_{\mathrm{r,cal},j}^{\mathrm{E}} - \varepsilon_{\mathrm{r,exp},j}^{\mathrm{E}} \right)^2 \right]^{1/2} \qquad (4)$$

where N is the number of $\varepsilon_{\mathrm{r,exp},j}^{\mathrm{E}}$ experimental data, and $\varepsilon_{\mathrm{r,cal},j}^{\mathrm{E}}$ is the corresponding value of the excess property $\varepsilon_{\mathrm{r}}^{\mathrm{E}}$ calculated from equation (3).

4. ERAS model

Some important features of this model are now given. (i) The excess functions are calculated as the sum of two contributions. The chemical contribution, $F_{\mathrm{m,chem}}^{\mathrm{E}}$, arises from hydrogen-bonding; the physical contribution, $F_{\mathrm{m,phys}}^{\mathrm{E}}$, is related to non-polar Van der Waals' interactions including free volume effects. Expressions for the molar excess functions $F_{\mathrm{m}}^{\mathrm{E}} = H_{\mathrm{m}}^{\mathrm{E}}$(enthalpy); $V_{\mathrm{m}}^{\mathrm{E}}$(volume) can be found elsewhere [38,39]. (ii) It is assumed that only consecutive linear association occurs. Such an association is described by a chemical

equilibrium constant (K_A) independent of the chain length of the associated species (amines), according to the equation:

$$A_m + A \leftrightarrow A_{m+1} \quad (5)$$

with m ranging from 1 to ∞. The cross-association between a self-associated species A_m and a non self-associated compound B (in this study, tertiary amides) is represented by

$$A_m + B \xleftrightarrow{K_{AB}} A_m B \quad (6)$$

Linear secondary amides (*N*-methylacetamide is also considered in this work) are also self-associated and their association is described by an equation similar to equation (5):

$$B_n + B \leftrightarrow B_{n+1} \quad (7)$$

with n ranging from 1 to ∞. The cross-association is then represented by:

$$A_m + B_n \xleftrightarrow{K_{AB}} A_m B_n \quad (8)$$

The cross-association constants (K_{AB}) of equations (6) and (8) are also considered to be independent of the chain length. Equations (5)-(8) are characterized by Δh_i^*, the enthalpy of the reaction that corresponds to the hydrogen-bonding energy, and by the volume change (Δv_i^*) related to the formation of the linear chains. (iii) The $F_{m,phys}^E$ term is derived from the Flory's equation of state [40], which is assumed to be valid not only for pure compounds but also for the mixture [41,42]:

$$\frac{\bar{P}_i \bar{V}_i}{\bar{T}_i} = \frac{\bar{V}_i^{1/3}}{\bar{V}_i^{1/3} - 1} - \frac{1}{\bar{V}_i \bar{T}_i} \quad (9)$$

where i = A,B or M (mixture). In equation (9), $\bar{V}_i = V_{mi} / V_i^*$; $\bar{P}_i = P / P_i^*$; $\bar{T}_i = T / T_i^*$ are the reduced properties for volume, pressure and temperature, respectively. The pure component reduction parameters V_i^* , P_i^* , T_i^* are obtained from *P-V-T* data (density, α_p , isobaric thermal expansion coefficient, and isothermal compressibility, κ_T), and association parameters [41,42]. The reduction parameters for the mixture P_M^* and T_M^* are calculated from mixing rules [41,42]. The total relative molecular volumes and surfaces of the compounds were calculated additively on the basis of the group volumes and surfaces recommended by Bondi [43].

4.1 Adjustment of ERAS parameters

Values of V_{mi}, V_i^* and P_i^* of pure compounds at T = 298.15 K, needed for calculations, are listed in Table S2 of supplementary material. K_A, Δh_A^*, and Δv_A^* of the self-associated amines and of *N*-methylacetamide are known from H_m^E and V_m^E data for the corresponding mixtures with alkanes [11-13,44]. The binary parameters to be fitted against H_m^E [18-20] and V_m^E [23,24,27,45] data available in the literature for amine + amide systems are then K_{AB}, Δh_{AB}^*, Δv_{AB}^* and X_{AB}. They are collected in Table 5.

4.2 Results

ERAS results are shown in Table 6 and Figures 5 and 6 (see also Figures S3 and S4 of supplementary material). We must underline that the model describes, rather correctly, the H_m^E and V_m^E functions of the amine + amide systems under study using parameters which smoothly change with the molecular structure. (Table 5).

5. Kirkwood-Fröhlich model

Some relevant hypotheses of the model are: (i) molecules of a given polar compound are assumed to be spherical (i.e., an intrinsic dipole moment inside a spherical cavity), (ii) the effect of the induced polarization of the molecules is treated in macroscopic way, assuming that the cavity is filled by a continuous medium of relative permittivity ε_r^∞ (the value of the permittivity at a high frequency at which only the induced polarizability contributes); (iii) long-range interactions are taken into account macroscopically by considering the outside of the cavity as a continuous dielectric of permittivity ε_r, leading to the Onsager local field; (iv) short-range interactions are not neglected. A central magnitude of the theory is the so-called Kirkwood correlation factor, g_K, which provides information of the deviations from randomness of the orientation of a dipole with respect to its neighbours. This is an important parameter, as it provides information on specific interactions in the liquid state. For a mixture, g_K can be determined, in the context of a one-fluid model [32], from macroscopic physical properties according to the expression [28,29,31,32]:

$$g_K = \frac{9k_B T V_m \varepsilon_0 (\varepsilon_r - \varepsilon_r^\infty)(2\varepsilon_r + \varepsilon_r^\infty)}{N_A \mu^2 \varepsilon_r (\varepsilon_r^\infty + 2)^2} \qquad (10)$$

Here, k_B is Boltzmann's constant; N_A, Avogadro's constant; ε_0, the vacuum permittivity; and V_m, the molar volume of the liquid at the working temperature, T. For polar compounds, ε_r^∞ is

estimated from the relation $\varepsilon_r^{\infty} = 1.1 n_D^2$ [46]. μ represents the gas phase dipole moment of the solution, estimated from the equation [32]:

$$\mu^2 = x_1 \mu_1^2 + x_2 \mu_2^2 \qquad (11)$$

where μ_i stands for the dipole moment of component i (=1,2) (Table 2).

The molar orientational polarizabilities (molar orientational polarizations or molar polarizability volumes), Π_m^{or}, are determined from [29-31]:

$$\Pi_m^{or} = \frac{N_A \alpha_{or}}{3\varepsilon_0} = \frac{(\varepsilon_r - \varepsilon_r^{\infty})(2\varepsilon_r + \varepsilon_r^{\infty})}{9\varepsilon_r} V_m \qquad (12)$$

where α_{or} stands for the orientational polarizability (in the case of mixtures, a one-fluid approach is implicit).

Molar induced polarizabilities, Π_m^{ind}, can be calculated in the framework of the Kirkwood-Fröhlich model by means of the expression:

$$\Pi_m^{ind} = \frac{N_A \alpha_{ind}}{3\varepsilon_0} = \frac{(\varepsilon_r^{\infty} - 1)(2\varepsilon_r + \varepsilon_r^{\infty})}{9\varepsilon_r} V_m \qquad (13)$$

with α_{ind} meaning the induced polarizability. Excess values of Π_m^{or} and Π_m^{ind} (Table 7, Figures 6 and S5, and S6 of supplementary material) have been obtained from the equation:

$$F^E = F - F^{id} \qquad (F = \Pi_m^{or} \text{ or } \Pi_m^{ind}) \qquad (14)$$

with F^{id} values determined from equations (12) or (13) using ideal values for the involved quantities in the mentioned equations. Particularly, calculations have been conducted using smoothed values of V_m^E [23,24,27,45], n_D [23,24,27] and ε_r^E (this work) at $\Delta x_1 = 0.01$.

6. Discussion

Along the present section, the values of the physical properties which involve some permittivity measurements and of their excess functions are referred to 298.15 K and $\phi_1 = 0.5$. Values of H_m^E and V_m^E are referred to 298.15 K and equimolar composition.

It is known that the disruption of interactions between like molecules, in the present case amide-amide and amine-amine interactions, contributes negatively to ε_r^E. For instance, the ε_r^E values of *n*-alkylamine + *n*-C_{12} systems at 293.15 K are: -0.314 (propylamine) < -0.243 (BA) < -0.133 (HxA) [47]. This negative contribution diminishes when increasing the chain length of the amine, as the amine group is then more sterically hindered, in such a way that the

effective polarity of longer amines becomes weaker. The creation of interactions between unlike molecules along the mixing process may lead either to a positive or to a negative contribution to ε_r^E [48]. A positive contribution is encountered when interactions between unlike molecules lead to an increased number of effective dipole moments in the system. Negative contributions arise when interactions between unlike molecules lead to a loss of the polar structure of the liquid, and therefore to a decreased number of effective dipole moments.

The large and negative ε_r^E values of DMA + linear amine mixtures reveal that the negative contributions from the breaking of interactions between like molecules are dominant. It is noteworthy that the ε_r^E values of *n*-alkylamine + *n*-C_{12} systems at 293.15 K are much less negative than those of DMA + *n*-alkylamine, e.g, -2.447 for the DPA system (see above). This suggests that ε_r^E of DMA solutions is determined, to a large extent, by the breaking of the dipolar interactions between DMA molecules. On the other hand, one can expect that interactions between unlike molecules contribute positively to ε_r^E. In fact, the ε_r^E value of the DMF + heptane mixture at $\phi_1 = 0.0171$ and 293.15 K is lower (– 0.24, calculated from data of the literature [49]) than the values of the corresponding systems with amines at the same conditions: – 0.129 (DPA), – 0.146 (DBA), – 0.104 (BA), and – 0.137 (HxA) [47]. Interestingly, ε_r^E is positive for the DMF + aniline mixture. This clearly indicates that ε_r^E is now mainly determined by the positive contribution related to the aniline-DMF interactions created upon mixing. Other systems as methanol + DMF (2.57 [50]); + DMA (0.52 [51]); + pyridine (2.85 [50]), or + cyclohexylamine (1.13 [52]) also show positive ε_r^E values.

We note that, in DMA solutions, ε_r^E(DBA) < ε_r^E(DPA) and ε_r^E(HxA) < ε_r^E(BA) (Table 7, Figures 1,2). This can be explained as follows: (i) longer amines are better breakers of the DMA-DMA interactions due to their large aliphatic surface; (ii) the formation of interactions between unlike molecules becomes easier when shorter amines are involved, as the amine group is then less sterically hindered. It is remarkable that ε_r^E(HxA) ≈ ε_r^E(DPA), which suggests that the ε_r decrease when HxA is replaced by DPA (note that ε_r^*(HxA) = 3.893 > ε_r^*(DPA) = 3.093, Table 2) is compensated by the creation of a larger number of interactions between unlike molecules in the case of the HxA mixture. Similar trends are observed for the corresponding systems with DMF, but an interesting difference is that ε_r^E(HxA) = -1.383 > ε_r^E(DPA) = -1.509 [25]. It seems that interactions between unlike molecules could be now even more important, as the amide group is less sterically hindered in DMF. Comparison between ε_r^E values of mixtures with a given linear amine shows that ε_r^E(DMF) > ε_r^E(DMA). In

addition, ε_r^E curves of the DMA systems are more skewed towards larger ϕ_1 values (Table 7). This suggests that linear amines can disrupt more easily DMA-DMA interactions and that the creation of amide-amine interactions is favoured when DMF molecules participate.

Finally, we must remark that the replacement of HxA ($\varepsilon_r^E = -1.383$) by aniline ($\varepsilon_r^E = 1.806$) in DMF solutions has a large impact on the ε_r^E values of these mixtures, which show opposite signs. Therefore, the aromaticity effect leads here to an increase of the number of effective dipole moments in the aniline system.

6.1 Temperature dependence of ε_r

Some important information on interactions and structure of a liquid can be inferred from the temperature dependence of ε_r. Of particular interest is the investigation of entropic effects induced in the liquid by the external electric field applied, $\vec{E}$. The relationship between $(\partial\varepsilon_r / \partial T)$ and the entropy increment per volume unit is given by [28,53-55]:

$$\frac{\Delta S}{\vec{E}^2} = \frac{S(T,\vec{E}) - S_0(T)}{\vec{E}^2} = \frac{\varepsilon_0}{2}\left(\frac{\partial \varepsilon_r}{\partial T}\right) \qquad (15)$$

In this expression, $S(T,\vec{E})$ is the entropy per volume unit of the system at temperature T under the application of $\vec{E}$, and $S_0(T)$ is the entropy per volume unit of the solution in absence of $\vec{E}$. The data analysis is more properly conducted on the basis of the $\frac{\Delta S}{\vec{E}^2}V_m$ magnitude as then one is considering along the discussion a number of molecules equal to N_A [54,55]. Within this treatment, volume variations with T have been neglected. We must note that $\Delta S < 0$ corresponds to the dipolar ordering action of $\vec{E}$, which is the normal behaviour of common liquids. All the pure compounds and systems along the present work follow this trend (Tables 2 and 8). From our results, some conclusions can be stated. (i) The molar entropy increments induced in amides are much more negative than those induced in amines (Table 2). This remarks the existence of strong dipolar interactions between amide molecules, which lead to the formation of entities of high polarity. Such entities are better oriented by the application of $\vec{E}$. (ii) For linear amines, the molar entropy increments become less negative in the sequence: BA > HxA > DPA > DBA (Table 2). Clearly, it can be ascribed to a meaningful decrease of the orientational polarizability of the amines in the same order (see below). Aniline shows the largest $\left|\frac{\Delta S}{\vec{E}^2}V_m\right|$ value, as a consequence of its stronger polar character. (iii) Interestingly, $\frac{\Delta S}{\vec{E}^2}V_m$ is more negative for DMA than for DMF (Table 2). This suggests that the ability of the DMA entities to respond to the ordering action of $\vec{E}$ is higher, a behavior that can be attributed to

weaker dipolar interactions between DMA molecules. This is supported experimentally by liquid-liquid equilibrium measurements, as the upper critical solution temperatures of heptane systems are 342.55 K (DMF) [56] > 309.8 K (DMA) [57] (see also the results from the Kirkwood-Fröhlich model below). (iv) A similar analysis is still valid for the considered mixtures (Table 8). For example, $\frac{\Delta S}{\vec{E}^2}V_m$ values of DMA solutions decrease in the sequence BA > DBA. This can be explained assuming, as previously, that DBA is a better breaker of interactions between amide molecules leading to a higher loss of the polar structure of DMA. This makes that the remaining DMA entities, of smaller size than those in pure amide, can be more easily oriented by the action of $\vec{E}$. It must be also remarked that the higher polar structure of the DMF + aniline system compared to that of the HxA system leads to a lower $\frac{\Delta S}{\vec{E}^2}V_m$ value for the former solution.

6.2 *Results from ERAS model*

The application of the ERAS model is useful to complete the description given above. Some important features are now given. (i) Amine-amide interactions are rather strong, as $\Delta h^*_{AB} = -22$ kJ·mol^{-1}, is a value not far from that used for 1-alkanol self-association (-25.1 kJ·mol^{-1}) in applications of the ERAS model [10,26,39,58]. It must be remarked that the same Δh^*_{AB} parameter is valid for all the tertiary amide + amine mixtures under consideration. (ii) Negative V^E_m values of BA, or DPA + DMA system arise from structural effects, as it is suggested by $V^E_{m,phys} < 0$ (Table 6) and positive X_{AB} values (Table 5). The $V^E_{m,chem}$ term (i.e., interactions between unlike molecules) is also relevant for the BA or DPA + DMF mixtures. Structural effects contribute more largely to V^E_m in DPA systems. (iii) The large $|V^E_{m,chem}|$ values of aniline mixtures may be indicative that the model overestimates this contribution. In fact, the V^E_m values of such systems are rather similar (V^E_m/cm^3·mol^{-1} = -0.662 (DMF) [27]; -0.636 (DMA) [45], T = 303.15 K), while the corresponding H^E_m values are very different (see above); (iv) The equilibrium constant K_{AB} decreases in the sequences: BA > HxA and DPA > DBA. In addition, for mixtures with a given amine, K_{AB} (DMF) > K_{AB} (DMA). If one takes into account that, in the ERAS model, self-association or solvation effects are described by means of linear chains formed by the system components, the relative variation of K_{AB} agrees with that encountered for ε^E_r. On the other hand, the large K_{AB} value for the DMF + aniline mixture is to be noted, as it remarks that interactions between unlike molecules become here rather important.

6.3 *Results from Kirkwood-Fröhlich's theory*

Firstly, we give values of $(\Pi_m^{or})^*$ and of $(\Pi_m^{ind})^*$ for pure compounds: $(\Pi_m^{or})^*$/ $cm^3 \cdot mol^{-1}$ = 623.0 (DMF); 773.0 (DMA); 68.0 (BA); 64.1 (HxA); 38.6 (DPA); 36.3 (DBA), 103.0 (aniline) and $(\Pi_m^{ind})^*/cm^3 \cdot mol^{-1}$ = 22.0 (DMF); 27.0 (DMA); 31.4 (BA); 45.7 (HXA); 47.9 (DPA); 63.0 (DBA), 42,7 (aniline). It is remarkable that $(\Pi_m^{or})^*$ of DMA is much larger than $(\Pi_m^{ind})^*$. It is also important to consider the sum of these two quantities (i.e. the total molar polarizability); in the same units: 645.0 (DMF); 800.0 (DMA); 99.4 (BA); 109.8 (HxA); 86.5 (DPA); 99.3 (DBA). These results indicate that DMA molecules are more easily oriented by the application of an electric field than DMF molecules, and underline that dipolar interactions between DMA molecules are weaker than in DMF. This was suggested by their $\frac{\Delta S}{\vec{E}^2} V_m$ values (see above). Interestingly, the total molar polarizability of the compounds does not vary in the same sense as ε_r^*. Nevertheless, it must be taken into account that, when applying a certain electric field, $(\varepsilon_r^* - 1)$ is proportional to the macroscopic dipole moment per unit volume, and therefore the trend of ε_r^* can be explained as arising from volume effects. In fact, the total molar polarizability per unit volume does vary accordingly to ε_r^*: 8.331 (DMF); 8.600 (DMA); 0.995 (BA); 0.825 (HxA); 0.627 (DPA); 0.580 (DBA); 1.54 (aniline).

Results for $(\Pi_m^{or})^E$ /(in $cm^3 \cdot mol^{-1}$) of DMA systems are: -42.6 (BA) > -56.4 (HxA) > -59.2 (DPA) > -69.5 (DBA). These $(\Pi_m^{or})^E$ values change in line with those of ε_r^E (Table 7), pointing out to a main contribution to ε_r^E arising from effects related to the orientational polarizability of the molecules. The same trend is observed for $(\Pi_m^{or})^E$ /$cm^3 \cdot mol^{-1}$ of DMF mixtures: 30.5 (aniline) > – 18.0 (BA) > – 27.8 (HxA) > – 31.6 (DPA) > – 41.4 (DBA). It seems to be clear that there is a loss of effective dipole moments in DMA + linear amines mixtures with regards to those involving DMF. In contrast, there is a meaningful increment of the effective dipole moments when HxA is replaced by aniline in DMF solutions. Interestingly, the $(\Pi_m^{ind})^E$ curves (Figures S5 and S6 of supplementary material) of *n*-alkylamine systems show a maximum at the concentrations where a minimum exists for the $(\Pi_m^{or})^E$ curves (Figure 6). This is a consistent result, as it indicates that the decrease of orientational polarization effects is linked to an increase of Π_m^{ind}, that is, roughly speaking, to an increase of dispersive interactions. For a given linear amine, the $(\Pi_m^{ind})^E$ maximum changes in the order: DMF < DMA, which also supports the more polar character of DMF solutions (Figures S5 and S6). In systems with a fixed amide, the mentioned maximum changes in the sequence: DBA > DPA > HxA > BA. That is, it decreases when the polarity of the mixture increases. It is to be noted that the increase of

polarity in the DMF + aniline system is accompanied by a decrease in the dispersive interactions (Figures 6 and S6, supplementary material).

The Balankina relative excess Kirkwood correlation factors [32], $g^{E}_{K,rel} = (g_K - g^{id}_K)/g^{id}_K$, where g_K and g^{id}_k account respectively for the real and ideal Kirkwood correlation factors, are a useful tool to probe into the structure of the mixtures:

$$g^{E}_{K,rel} = \frac{V_m(\varepsilon_r - \varepsilon_r^{\infty})(2\varepsilon_r + \varepsilon_r^{\infty})\varepsilon_r^{id}(\varepsilon_r^{id,\infty} + 2)^2}{V_m^{id}(\varepsilon_r^{id} - \varepsilon_r^{id,\infty})(2\varepsilon_r^{id} + \varepsilon_r^{id,\infty})\varepsilon_r(\varepsilon_r^{\infty} + 2)^2} - 1 \qquad (16)$$

It is also possible to develop a two-liquid model [32], in which liquid i (i=1,2) is defined by molecules of pure substance i located in spherical cavities of volume $\bar{V}_{mi}/N_A$ (where $\bar{V}_{mi}$ stands for the partial molar volume of component i) and embedded in a dielectric continuum formed by the real mixture at the same composition. This approach leads to the definition of the relative excess Kirkwood correlation factor of liquid i, which is given by:

$$g^{E}_{K,rel,i} = \frac{\bar{V}_{mi}(\varepsilon_r - \varepsilon_{ri}^{\infty})(2\varepsilon_r + \varepsilon_{ri}^{\infty})\varepsilon_r^{id}}{V_{mi}(\varepsilon_r^{id} - \varepsilon_r^{\infty})(2\varepsilon_r^{id} + \varepsilon_{ri}^{\infty})\varepsilon_r} - 1 \qquad (17)$$

Values of $g^{E}_{K,rel}$ and $g^{E}_{K,rel,i}$ are collected in Table 7 (Figures 7-10). From inspection of the results obtained some conclusions regarding systems with linear amines can be stated. (i) The $g^{E}_{K,rel}$ values are negative over the whole composition range. As in the ideal mixture neither correlations between like dipoles are destroyed nor are new correlations between unlike dipoles created, these results show that there is a destruction of the structure in the solution with regards to that of the ideal mixture. (ii) Interestingly, the $g^{E}_{K,rel}$ curves are skewed towards low ϕ_1 values (Figures 7 and 8). This suggests that the amide structure is better destroyed at such concentrations. (iii) An interesting result is that the minima of the $g^{E}_{K,rel}$ curves is reached at lower volume fractions of the amide than in the ε_r^{E} and $(\Pi_m^{or})^{E}$ curves (Table 7). Thus, according to the Kirkwood-Fröhlich model, the destruction of dipole correlations is not the only responsible for the ε_r^{E} minima, but other related effects, such as the number and strength of interactions created and disrupted upon mixing, are also important. (iv) The minimum values change in similar order to that encountered for ε_r^{E}. For example, $g^{E}_{K,rel}$ (DMA) = -0.14 (BA) > -0.18 (HxA) > -0.21 (DPA) > -0.24 (DBA). The BA mixture is the most structured, which can be ascribed to a higher relevance of the creation of interactions between unlike molecules. (v) Similarly, systems with DMF are also more structured than those with DMA. (vi) For a given mixture, the $g^{E}_{K,rel,i}$ values are practically independent of the component considered and are similar to $g^{E}_{K,rel}$ values (Table 7). This may mean than interaction between unlike molecules

partially compensate the loss of structure of the components. (vi) The $\left|g^{E}_{K,rel,1}\right|$ values are larger for DMA than for DMF in systems with a given linear amine. That is, the loss of order in the liquid state is higher in the vicinity of a DMA molecule than around a DMF molecule.

Finally, we must remark the positive values of $g^{E}_{K,rel}$ and $g^{E}_{K,rel,i}$ for the DMF + aniline mixture. They show that the passage from an ideal to a real mixture leads here to an increment of the order in the liquid state, which, in addition, is higher in the neighbourhood of the aniline molecules. The DMF + HxA system behaves in the opposite way and there is a loss of order in the liquid state when passing from an ideal to a real mixture.

7. Conclusions

Measurements on ε_r have been reported for the systems: DMA + BA, + HxA, + DPA, or + DBA and for DMF + aniline at (293.15-303.15) K. The corresponding ε_r^E values are large and negative for mixtures with linear amines and positive for the aniline solution. In the former case, this means that the main contributions to ε_r^E come from the disruption of interactions between like molecules. In the latter case, the ε_r^E sign is determined by the positive contribution from the DMF-aniline interactions. Inspection of ε_r^E data shows that: (i) longer linear amines are better breakers of the amide-amide interactions; (ii) interactions between unlike molecules are more easily formed when shorter linear amines, or DMF, participate. Calculations on $(\Pi_m^{or})^E$, $(\Pi_m^{ind})^E$, $g^E_{K,rel}$ and $g^E_{K,rel,i}$, and the dependence of K_{AB} with the molecular structure are consistent with these findings.

Acknowledgements

The authors gratefully acknowledge the financial support received from the Consejería de Educación y Cultura of Junta de Castilla y León, under Project BU034U16. F. Hevia and A. Cobos are grateful to Ministerio de Educación, Cultura y Deporte for the grants FPU14/04104 and FPU15/05456 respectively.

References

[1] E.S. Eberhardt, R.T. Raines, J. Am. Chem. Soc. 116 (1994) 2149-2150.

[2] A.L. McClellan, Tables of Experimental Dipole Moments, Vols. 1,2,3, Rahara Enterprises, El Cerrito, US, 1974.

[3] J.A. Riddick, W.B. Bunger, T.K. Sakano, Organic solvents: physical properties and methods of purification, Wiley, New York, 1986.

[4] W.L. Jorgensen, C.J. Swenson, J. Am. Chem. Soc. 107 (1985) 569-578.

[5] J.A. Gonzalez, J.C. Cobos, I. García de la Fuente, Fluid Phase Equilib. 224 (2004) 169-183.

[6] J. Barthel, R. Buchner, B. Wurm, J. Mol. Liq. 98 (2002) 51-69.

[7] F.F. Liew, T. Hasegawa, M. Fukuda, E. Nakata, T. Morii, Bioorg. Med. Chem. 19 (2011) 4473-4481.

[8] J.M. Sonner, R.S. Cantor, Annu. Rev. Biophys. 42 (2013) 143-167.

[9] D.L. Nelson, M.M. Cox, Lehninger Principles of Biochemistry, 3rd ed., Worth Publishing, New York, 2000.

[10] H. Funke, M. Wetzel, A. Heintz, Pure Appl. Chem. 61 (1989) 1429-1439.

[11] S. Villa, J.A. González, I.G. De La Fuente, N. Riesco, J.C. Cobos, J. Solution Chem. 31 (2002) 1019-1038.

[12] J.A. González, I. Mozo, I. García de la Fuente, J.C. Cobos, Can. J. Chem. 83 (2005) 1812-1825.

[13] S. Villa, N. Riesco, I. García de la Fuente, J.A. González, J.C. Cobos, Fluid Phase Equilib. 216 (2004) 123-133.

[14] J.A. González, L.F. Sanz, I. García De La Fuente, J.C. Cobos, Thermochim. Acta 573 (2013) 229-236.

[15] R.C. Reid, J.M. Prausnitz, B.E. Poling, The Properties of Gases and Liquids, McGraw-Hill, New York, US, 1987.

[16] H. Matsuda, K. Ochi, K. Kojima, J. Chem. Eng. Data 48 (2003) 184-189.

[17] T.W. Whitfield, G.J. Martyna, S. Allison, S.P. Bates, H. Vass, J. Crain, J. Phys. Chem. B 110 (2006) 3624-3637.

[18] R.S. Ramadevi, P. Venkatesu, M.V. Prabhakara Rao, M.R. Krishna, Fluid Phase Equilib. 114 (1996) 189-197.

[19] G. Chandra Sekhar, M.V. Prabhakara Rao, D.H.L. Prasad, Y.V.L. Ravi Kumar, Thermochim. Acta 402 (2003) 99-103.

[20] A.B. de Haan, J. Gmehling, J. Chem. Eng. Data 41 (1996) 474-478.

[21] L. Pikkarainen, J. Solution Chem. 16 (1987) 125-132.

[22] M. Oba, S. Murakami, R. Fujishiro, J. Chem. Thermodyn. 9 (1977) 407-414.

[23] F. Hevia, A. Cobos, J.A. González, I. García de la Fuente, L.F. Sanz, J. Chem. Eng. Data 61 (2016) 1468-1478.

[24] F. Hevia, A. Cobos, J.A. González, I.G. de la Fuente, V. Alonso, J. Solution Chem. 46 (2017) 150-174.

[25] F. Hevia, J.A. González, I. García de la Fuente, L.F. Sanz, J.C. Cobos, J. Mol. Liq. 238 (2017) 440-446.

[26] A. Heintz, Ber. Bunsenges. Phys. Chem. 89 (1985) 172-181.

[27] H.J. Noh, S.J. Park, S.J. In, J. Ind. Eng. Chem. 16 (2010) 200-206.

[28] H. Fröhlich, Theory of Dielectrics, Clarendon Press, Oxford, 1958.

[29] C. Moreau, G. Douhéret, J. Chem. Thermodyn. 8 (1976) 403-410.

[30] P. Bordewijk, Physica 69 (1973) 422-432.

[31] A. Chelkowski, Dielectric Physics, Elsevier, Amsterdam, 1980.

[32] J.C.R. Reis, T.P. Iglesias, Phys. Chem. Chem. Phys. 13 (2011) 10670-10680.

[33] CIAAW, ciaaw.org/atomic-weights.htm (accessed 2015).

[34] V. Alonso, J.A. González, I. García de la Fuente, J.C. Cobos, Thermochim. Acta 543 (2012) 246-253.

[35] J.C.R. Reis, T.P. Iglesias, G. Douhéret, M.I. Davis, Phys. Chem. Chem. Phys. 11 (2009) 3977-3986.

[36] A. Chaudhari, C.S. Patil, A.G. Shankarwar, B.R. Arbad, S.C. Mehrotra, J. Korean Chem. Soc. 45 (2001) 201-206.

[37] P.R. Bevington, D.K. Robinson, Data Reduction and Error Analysis for the Physical Sciences, McGraw-Hill, New York, 2000.

[38] J.A. González, S. Villa, N. Riesco, I. García de la Fuente, J.C. Cobos, Can. J. Chem. 81 (2003) 319-329.

[39] J.A. González, I. García de la Fuente, J.C. Cobos, Fluid Phase Equilib. 168 (2000) 31-58.

[40] P.J. Flory, J. Am. Chem. Soc. 87 (1965) 1833-1838.

[41] A. Heintz, P.K. Naicker, S.P. Verevkin, R. Pfestorf, Ber. Bunsenges. Phys. Chem. 102 (1998) 953-959.

[42] A. Heintz, D. Papaioannou, Thermochim. Acta 310 (1998) 69-76.

[43] A. Bondi, Physical Properties of Molecular Crystals, Liquids and Glasses, Wiley, New York, 1968.

[44] J.A. González, Phys. Chem. Liq. 42 (2004) 159-172.

[45] G. Chandrasekhar, P. Venkatesu, M.V. Prabhakara Rao, Phys. Chem. Liq. 40 (2002) 181-189.

[46] Y. Marcus, J. Solution Chem. 21 (1992) 1217-1230.

[47] S. Otín, J. Fernández, J.M. Embid, I. Velasco, C.G. Losa, Ber. Bunsenges. Phys. Chem. 90 (1986) 1179-1183.

[48] J.A. González, L.F. Sanz, I. García de la Fuente, J.C. Cobos, J. Chem. Thermodyn. 91 (2015) 267-278.

[49] C. Wohlfahrt, Static Dielectric Constants of Pure Liquids and Binary Liquid Mixtures. Landolt-Börnstein - Group IV Physical Chemistry Vol. 6, Springer Berlin Heidelberg, Berlin, 1991.

[50] M.S. Bakshi, G. Kaur, J. Chem. Eng. Data 42 (1997) 298-300.

[51] G. Ritzoulis, A. Fidantsi, J. Chem. Eng. Data 45 (2000) 207-209.

[52] L.F. Sanz, J.A. González, I.G. De La Fuente, J.C. Cobos, Thermochim. Acta 631 (2016) 18-27.

[53] J. Jadżyn, G. Czechowski, J.-L. Déjardin, M. Ginovska, J. Phys. Chem. A 111 (2007) 8325-8329.

[54] J. Świergiel, I. Płowaś, J. Jadżyn, J. Mol. Liq. 220 (2016) 879-882.

[55] J. Świergiel, I. Płowaś, J. Jadżyn, J. Mol. Liq. 223 (2016) 628-634.

[56] J. Lobos, I. Mozo, M. Fernández Regúlez, J.A. González, I. García de la Fuente, J.C. Cobos, J. Chem. Eng. Data 51 (2006) 623-627.

[57] X. An, H. Zhao, F. Jiang, W. Shen, J. Chem. Thermodyn. 28 (1996) 1221-1232.

[58] J.A. González, I. Alonso, C. Alonso-Tristán, I.G.D.L. Fuente, J.C. Cobos, J. Chem. Thermodyn. 56 (2013) 89-98.

[59] J. Barthel, K. Bachhuber, R. Buchner, J.B. Gill, M. Kleebauer, Chem. Phys. Lett. 167 (1990) 62-66.

[60] P. Undre, S.N. Helambe, S.B. Jagdale, P.W. Khirade, S.C. Mehrotra, J. Mol. Liq. 137 (2008) 147-151.

[61] T. Yokoyama, E. Iwamoto, T. Kumamaru, Bull. Chem. Soc. Jpn. 64 (1991) 1198-1204.

[62] R.J. Sengwa, V. Khatri, Thermochim. Acta 506 (2010) 47-51.

[63] J. Świergiel, J. Jadżyn, J. Chem. Eng. Data 54 (2009) 2296-2300.

[64] C.M. Kinart, W.J. Kinart, Phys. Chem. Liq. 31 (1996) 1-8.

[65] R.J. Sengwa, Madhvi, S. Sankhla, Phys. Chem. Liq. 44 (2006) 637-653.

[66] R.J. Sengwa, S. Sankhla, V. Khatri, Fluid Phase Equilib. 285 (2009) 50-53.

[67] C.M. Kinart, A. Ćwiklińska, W.J. Kinart, A. Bald, J. Chem. Eng. Data 49 (2004) 1425-1428.

[68] F. Ratkovics, L. Domonkos, Acta Chim. Acad. Sci. Hung. 89 (1976) 325.

[69] F.J. Arcega Solsona, J.M. Fornies-Marquina, J. Phys. D: Appl. Phys. 15 (1982) 1783-1793.

[70] C.M. Kinart, W.J. Kinart, D. Chęcińska-Majak, J. Chem. Eng. Data 48 (2003) 1037-1039.

[71] S. Murakami, R. Fujishiro, Bull. Chem. Soc. Jpn. 39 (1966) 720-725.

[72] V.A. Rana, A.D. Vyas, S.C. Mehrotra, J. Mol. Liq. 102 (2003) 379-391.

[73] S.P. Patil, A.S. Chaudhari, M.P. Lokhande, M.K. Lande, A.G. Shankarwar, S.N. Helambe, B.R. Arbad, S.C. Mehrotra, J. Chem. Eng. Data 44 (1999) 875-878.

[74] S. Lata, K.C. Singh, A. Suman, J. Mol. Liq. 147 (2009) 191-197.

[75] B.D. Watode, P.G. Hudge, M.N. Shinde, R.B. Talware, A.C. Kumbharkhane, Phys. Chem. Liq. 53 (2015) 252-263.

[76] A.N. Prajapati, V.A. Rana, A.D. Vyas, Ind. J. Pure Appl. Phys. 51 (2013) 104-111.

[77] G. Parthipan, T. Thenappan, J. Mol. Liq. 138 (2008) 20-25.

[78] T.V. Krishna, S.S. Sastry, J. Solution Chem. 39 (2010) 1377-1393.

[79] P.S. Nikam, S.J. Kharat, J. Chem. Eng. Data 48 (2003) 972-976.

Table 1

Sample description.

Chemical name	CAS Number	Source	Purification method	Purity[a]
N,N-dimethylacetamide (DMA)	127-19-5	Sigma-Aldrich	None	0.9998
N,N-dimethylformamide (DMF)	68-12-2	Sigma-Aldrich	None	0.9995
N-propylpropan-1-amine (DPA)	142-84-7	Aldrich	None	0.996
N-butylbutan-1-amine (DBA)	111-92-2	Aldrich	None	0.9974
butan-1-amine (BA)	109-73-9	Sigma-Aldrich	None	0.9996
Hexan-1-amine (HxA)	111-26-2	Aldrich	None	0.999
Aniline	62-53-3	Sigma-Aldrich	None	0.999

[a] In mole fraction. Provided by the supplier by gas chromatography.

Table 2

Relative permittivity, ε_r^*, of pure compounds at temperature T, pressure p = 0.1 MPa and frequency $\nu = 1$ MHz. [a]

Compound[b]	T/K	ε_r^*		$V_m \frac{\partial \varepsilon_r^*}{\partial T}$ / cm^3·mol^{-1}·K^{-1}	μ /D
		Exp.	Lit.		
DMA	293.15	39.695			
	298.15	38.586	38.60 [59]; 43.00 [60], 37.78 [61]	−20.47 [c]	3.7 [2]
	303.15	37.499	37.72 [62]; 38.67 [63]		
DMF	293.15	38.334	38.30 [64]		
	298.15	37.440	37.65 [65], 37.6 [50]	−13.55 [d]	3.7 [3]
	303.15	36.580	36.55 [66]		
DPA	293.15	3.148	3.31 [67]; 3.068 [3]		
	298.15	3.093	3.24 [67]	−1.52 [c]	1.0 [15]
	303.15	3.037	3.18 [3]		
DBA	293.15	2.938	2.978 [3]; 2.765 [68]		
	298.15	2.896		−1.37 [c]	1.1 [15]
	303.15	2.858	2.697 [68]		
BA	293.15	4.729	4.71 [69]; 4.88 [3]; 4.91 [70]; 5.34 [71]; 4.70 [47]		
	298.15	4.636	4.62 [70]; 5.16 [71]	−1.90 [c]	1.3 [15]
	303.15	4.547	4.57 [70]; 4.48 [71]		
HxA	293.15	3.955	3.94 [47]		
	298.15	3.893		−1.73 [c]	1.3 [2]
	303.15	3.835	3.83 [47]		
Aniline [e]	293.15	7.117	6.48 [72]; 6.55 [73]		
	298.15	6.984	6.774 [74], 6.59 [75]	−2.39[e]	1.51 [3]
	303.15	6.856	6.09 [72]; 6.0 [73]; 6.71 [3]; 6.88 [76]; 6.857 [77]; 6.055 [78]		

[a]The standard uncertainties are: $u(T) = 0.02$ K; $u(p) = 1$ kPa; $u(\nu) = 20$ Hz. The total relative standard uncertainty is: $u_r(\varepsilon_r^*) = 0.003$; [b]for symbols, see Table 1; [c]molar volume, V_m, taken from ref. [24]; [d] V_m taken from ref. [23]; [e] V_m taken from Table S1.

Table 3

Volume fractions of amide, ϕ_1, relative permittivities, ε_r, and excess relative permittivities, ε_r^E, of DMA (1) + amine (2) and and DMF (1) + aniline (2)[a] mixtures as functions of the mole fraction of amide, x_1, at temperature T, pressure p = 0.1 MPa and frequency $\nu = 1$ MHz. [b]

x_1	ϕ_1	ε_r	ε_r^E	x_1	ϕ_1	ε_r	ε_r^E
DMA (1) + DPA (2) ; T/K = 293.15							
0.0000	0.0000	3.148		0.6398	0.5453	20.725	– 2.352
0.0600	0.0413	4.165	– 0.492	0.6985	0.6100	23.242	– 2.200
0.1099	0.0769	5.107	– 0.851	0.7479	0.6670	25.568	– 1.957
0.1494	0.1060	5.897	– 1.125	0.7948	0.7234	27.856	– 1.730
0.2122	0.1539	7.264	– 1.509	0.8464	0.7881	30.535	– 1.416
0.3021	0.2261	9.460	– 1.951	0.8928	0.8490	33.134	– 1.042
0.4041	0.3140	12.353	– 2.271	0.9494	0.9268	36.494	– 0.526
0.4917	0.3951	15.141	– 2.447	1.0000	1.0000	39.695	
0.5905	0.4933	18.754	– 2.423				
DMA (1) + DPA (2) ; T/K = 298.15							
0.0000	0.0000	3.093		0.6398	0.5450	20.156	– 2.281
0.0600	0.0413	4.083	– 0.476	0.6985	0.6097	22.613	– 2.120
0.1099	0.0768	4.990	– 0.829	0.7479	0.6667	24.852	– 1.904
0.1494	0.1059	5.757	– 1.095	0.7948	0.7231	27.082	– 1.676
0.2122	0.1537	7.088	– 1.460	0.8464	0.7879	29.694	– 1.364
0.3021	0.2259	9.217	– 1.894	0.8928	0.8488	32.205	– 1.014
0.4041	0.3138	12.018	– 2.213	0.9494	0.9267	35.464	– 0.520
0.4917	0.3947	14.741	– 2.361	1.0000	1.0000	38.586	
0.5905	0.4930	18.239	– 2.352				
DMA (1) + DPA (2) ; T/K = 303.15							
0.0000	0.0000	3.037		0.6398	0.5446	19.598	– 2.207
0.0600	0.0412	3.999	– 0.458	0.6985	0.6094	21.993	– 2.045
0.1099	0.0768	4.873	– 0.811	0.7479	0.6664	24.135	– 1.867
0.1494	0.1058	5.619	– 1.064	0.7948	0.7229	26.324	– 1.626
0.2122	0.1535	6.912	– 1.415	0.8464	0.7877	28.874	– 1.309
0.3021	0.2257	8.980	– 1.835	0.8928	0.8487	31.293	– 0.992
0.4041	0.3135	11.690	– 2.151	0.9494	0.9267	34.462	– 0.511
0.4917	0.3944	14.338	– 2.291	1.0000	1.0000	37.499	

TABLE 3 (continued)

0.5905	0.4926	17.732	– 2.281				
DMA (1) + DBA (2) ; *T*/K = 293.15							
0.0000	0.0000	2.938		0.6015	0.4510	16.820	– 2.695
0.0896	0.0508	4.186	– 0.619	0.6429	0.4949	18.472	– 2.657
0.1507	0.0881	5.155	– 1.021	0.7094	0.5706	21.390	– 2.522
0.2190	0.1324	6.372	– 1.433	0.7469	0.6163	23.221	– 2.370
0.3109	0.1971	8.266	– 1.917	0.7992	0.6842	25.981	– 2.106
0.3974	0.2641	10.350	– 2.296	0.8428	0.7448	28.506	– 1.809
0.4353	0.2956	11.384	– 2.419	0.8963	0.8247	31.920	– 1.331
0.4940	0.3470	13.117	– 2.576	0.9456	0.9044	35.389	– 0.792
0.5505	0.4000	14.971	– 2.670	1.0000	1.0000	39.695	
DMA (1) + DBA (2) ; *T*/K = 298.15							
0.0000	0.0000	2.896		0.6015	0.4509	16.376	– 2.613
0.0896	0.0508	4.106	– 0.603	0.6429	0.4948	17.967	– 2.588
0.1507	0.0880	5.045	– 0.992	0.7094	0.5704	20.804	– 2.450
0.2190	0.1323	6.224	– 1.394	0.7469	0.6161	22.565	– 2.320
0.3109	0.1970	8.063	– 1.864	0.7992	0.6840	25.246	– 2.062
0.3974	0.2640	10.085	– 2.233	0.8428	0.7446	27.715	– 1.756
0.4353	0.2954	11.084	– 2.355	0.8963	0.8246	31.031	– 1.295
0.4940	0.3468	12.766	– 2.507	0.9456	0.9043	34.398	– 0.772
0.5505	0.3998	14.575	– 2.590	1.0000	1.0000	38.586	
DMA (1) + DBA (2) ; *T*/K = 303.15							
0.0000	0.0000	2.858		0.6015	0.4507	15.942	– 2.529
0.0896	0.0508	4.033	– 0.585	0.6429	0.4946	17.504	– 2.487
0.1507	0.0880	4.942	– 0.964	0.7094	0.5703	20.253	– 2.361
0.2190	0.1323	6.086	– 1.355	0.7469	0.6160	21.966	– 2.231
0.3109	0.1970	7.871	– 1.811	0.7992	0.6839	24.579	– 1.970
0.3974	0.2639	9.833	– 2.167	0.8428	0.7446	26.984	– 1.668
0.4353	0.2953	10.809	– 2.278	0.8963	0.8245	30.209	– 1.211
0.4940	0.3467	12.440	– 2.428	0.9456	0.9043	33.491	– 0.693
0.5505	0.3997	14.195	– 2.509	1.0000	1.0000	37.499	
DMA (1) + BA (2) ; *T*/K = 293.15							
0.0000	0.0000	4.729		0.5989	0.5822	23.127	– 1.935
0.0584	0.0547	6.126	– 0.513	0.6947	0.6798	26.781	– 1.689

TABLE 3 (continued)

0.1069	0.1005	7.365	– 0.874	0.7906	0.7789	30.606	– 1.325
0.1973	0.1866	9.841	– 1.405	0.8404	0.8309	32.664	– 1.083
0.3034	0.2890	13.000	– 1.822	0.8970	0.8904	35.070	– 0.755
0.4037	0.3872	16.238	– 2.014	0.9491	0.9457	37.354	– 0.403
0.4978	0.4805	19.477	– 2.033	1.0000	1.0000	39.653	
DMA (1) + BA (2) ; *T*/K = 298.15							
0.0000	0.0000	4.636		0.5989	0.5818	22.511	– 1.842
0.0584	0.0546	5.989	– 0.497	0.6947	0.6795	26.066	– 1.598
0.1069	0.1003	7.194	– 0.841	0.7906	0.7786	29.779	– 1.244
0.1973	0.1863	9.596	– 1.354	0.8404	0.8307	31.779	– 1.009
0.3034	0.2887	12.665	– 1.755	0.8970	0.8903	34.105	– 0.703
0.4037	0.3868	15.823	– 1.922	0.9491	0.9456	36.315	– 0.367
0.4978	0.4801	18.954	– 1.953	1.0000	1.0000	38.526	
DMA (1) + BA (2) ; *T*/K = 303.15							
0.0000	0.0000	4.547		0.5989	0.5814	21.946	– 1.769
0.0584	0.0545	5.863	– 0.481	0.6947	0.6791	25.392	– 1.544
0.1069	0.1002	7.034	– 0.816	0.7906	0.7784	28.998	– 1.211
0.1973	0.1861	9.380	– 1.302	0.8404	0.8304	30.943	– 0.981
0.3034	0.2883	12.352	– 1.700	0.8970	0.8901	33.220	– 0.672
0.4037	0.3864	15.431	– 1.855	0.9491	0.9455	35.362	– 0.356
0.4978	0.4797	18.478	– 1.884	1.0000	1.0000	37.515	
DMA (1) + HxA (2) ; *T*/K = 293.15							
0.0000	0.0000	3.955		0.6944	0.6138	23.705	– 2.183
0.1027	0.0741	5.810	– 0.793	0.7581	0.6867	26.548	– 1.945
0.1921	0.1426	7.690	– 1.361	0.8028	0.7401	28.677	– 1.724
0.3016	0.2320	10.349	– 1.896	0.8528	0.8021	31.226	– 1.390
0.3994	0.3175	13.099	– 2.201	0.8986	0.8611	33.671	– 1.054
0.5066	0.4180	16.508	– 2.383	0.9529	0.9340	36.812	– 0.518
0.6030	0.5151	20.011	– 2.350	1.0000	1.0000	39.688	
DMA (1) + HxA (2) ; *T*/K = 298.15							
0.0000	0.0000	3.893		0.6944	0.6137	23.075	– 2.118
0.1027	0.0741	5.694	– 0.771	0.7581	0.6866	25.835	– 1.888
0.1921	0.1425	7.522	– 1.317	0.8028	0.7400	27.897	– 1.679
0.3016	0.2319	10.096	– 1.846	0.8528	0.8020	30.358	– 1.370

TABLE 3 (continued)

0.3994	0.3173	12.772	– 2.134	0.8986	0.8610	32.742	– 1.034
0.5066	0.4178	16.083	– 2.311	0.9529	0.9340	35.798	– 0.511
0.6030	0.5150	19.493	– 2.274	1.0000	1.0000	38.600	
DMA (1) + HxA (2) ; *T*/K = 303.15							
0.0000	0.0000	3.835		0.6944	0.6135	22.498	– 2.022
0.1027	0.0740	5.588	– 0.742	0.7581	0.6864	25.163	– 1.815
0.1921	0.1424	7.362	– 1.274	0.8028	0.7398	27.182	– 1.597
0.3016	0.2317	9.866	– 1.781	0.8528	0.8019	29.567	– 1.306
0.3994	0.3172	12.465	– 2.065	0.8986	0.8609	31.893	– 0.969
0.5066	0.4177	15.690	– 2.229	0.9529	0.9339	34.820	– 0.503
0.6030	0.5148	19.005	– 2.188	1.0000	1.0000	37.552	
DMF (1) + aniline (2) ; *T*/K = 293.15							
0.0000	0.0000	7.117		0.5999	0.5589	26.184	1.620
0.0533	0.0454	8.910	0.376	0.6989	0.6624	28.955	1.160
0.1046	0.0899	10.653	0.730	0.7931	0.7641	31.604	0.634
0.1562	0.1353	12.414	1.073	0.8431	0.8195	33.120	0.421
0.2033	0.1774	14.004	1.349	0.8982	0.8818	34.833	0.189
0.3015	0.2673	17.269	1.808	0.9459	0.9366	36.439	0.084
0.4071	0.3672	20.625	2.045	1.0000	1.0000	38.334	
0.5013	0.4593	23.428	1.973				
DMF (1) + aniline (2) ; *T*/K = 298.15							
0.0000	0.0000	6.984		0.5999	0.5592	25.601	1.586
0.0533	0.0455	8.729	0.359	0.6989	0.6626	28.310	1.146
0.1046	0.0899	10.426	0.704	0.7931	0.7643	30.920	0.658
0.1562	0.1354	12.144	1.036	0.8431	0.8197	32.402	0.453
0.2033	0.1775	13.689	1.299	0.8982	0.8819	34.071	0.228
0.3015	0.2675	16.874	1.743	0.9459	0.9367	35.620	0.108
0.4071	0.3674	20.146	1.972	1.0000	1.0000	37.440	
0.5013	0.4596	22.895	1.913				
DMF (1) + aniline (2) ; *T*/K = 303.15							
0.0000	0.0000	6.856		0.5999	0.5593	25.026	1.545
0.0533	0.0455	8.557	0.349	0.6989	0.6627	27.687	1.133
0.1046	0.0900	10.200	0.669	0.7931	0.7644	30.246	0.669
0.1562	0.1355	11.876	0.992	0.8431	0.8198	31.690	0.466

TABLE 3 (continued)

0.2033	0.1777	13.383	1.245	0.8982	0.8819	33.315	0.245
0.3015	0.2676	16.485	1.675	0.9459	0.9367	34.821	0.123
0.4071	0.3676	19.678	1.895	1.0000	1.0000	36.580	
0.5013	0.4597	22.371	1.851				

[a]For symbols, see Table 1; [b]The standard uncertainties are: $u(T) = 0.02$ K; $u(p) = 1$ kPa; $u(\nu) = 20$ Hz; $u(x_1) = 0.0010$; $u(\phi_1) = 0.0040$. The relative standard uncertainty is: $u_r(\varepsilon_r) = 0.003$; and the relative combined expanded uncertainty (0.95 level of confidence) is $U_{rc}(\varepsilon_r^E) = 0.03$.

Table 4

Coefficients A_i and standard deviations, $\sigma\left(\varepsilon_r^E\right)$ (equation (4)), for the representation of ε_r^E at temperature T and pressure p = 0.1 MPa for DMA (1) + amine (2) and DMF (1) + aniline (2) systems by equation (3).

System[a]	T/K	A_0	A_1	A_2	A_3	A_4	$\sigma\left(\varepsilon_r^E\right)$
DMA + DPA	293.15	– 9.79	– 1.40				0.012
	298.15	– 9.50	– 1.34				0.007
	303.15	– 9.21	– 1.30				0.007
DMA + DBA	293.15	– 10.35	– 4.09	– 1.03			0.011
	298.15	– 10.06	– 4.00	– 1.06			0.009
	303.15	– 9.76	– 3.70	– 0.69			0.006
DMA + BA	293.15	– 8.16	0.72	– 0.81			0.008
	298.15	– 7.81	0.86	– 0.64			0.006
	303.15	– 7.53	0.83	– 0.67			0.008
DMA + HxA	293.15	– 9.49	– 1.70	– 0.9			0.010
	298.15	– 9.19	– 1.68	– 1.0			0.012
	303.15	– 8.86	– 1.52	– 0.9			0.011
DMF + aniline	293.15	7.87	– 4.1	– 5.6	1.0	1.7	0.012
	298.15	7.63	– 3.83	– 5.2	1.2	1.7	0.010
	303.15	7.38	– 3.48	– 4.8	1.2	1.7	0.009

[a]For symbols, see Table 1

Table 5

ERAS parameters[a] for amine (1) + amide (2) mixtures at 298.15 K.

System[b]	K_{AB}	Δh^*_{AB} / kJ·mol^{-1}	Δv^*_{AB} / cm^3·mol^{-1}	X_{AB} / J·cm^{-3}
BA + DMF	1.2	−22	−2.5	10
HxA + DMF	0.65	−22	−2.5	10
DPA + DMF	0.6	−22	−3.1	10
DBA + DMF	0.20	−22	−3.1	17.45
BA + DMA	0.75	−22	−2.5	10
HxA + DMA	0.50	−22	−2.5	10
DPA + DMA	0.25	−22	−3.9	10
DBA + DMA	0.12	−22	−3.9	17.45
Aniline + DMF	70	−22	−11.1	4
Aniline + DMA	2.20	−22	−20	3.2
HxA + NMA[c]	20	−25.	−3.2	5

[a] K_{AB}, association constant of component A with component B; Δh^*_{AB}, association enthalpy of component A with component B; Δv^*_{AB}, association volume of component A with component B; X_{AB}, physical parameter; [b]for symbols, see Table 1; [c]T = 363.15 K.

Table 6

Excess molar volumes, V_m^E, at 298.15, equimolar composition and 0.1 MPa for amine (1) + *N,N*-dialkylamide (2) mixtures. Comparison of experimental results (exp) with ERAS calculations; the physical ($V_{m,phys}^E$) and chemical ($V_{m,chem}^E$) contributions are also listed.

System[a]	V_m^E				Ref.
	Exp.	ERAS[b]	$V_{m,phys}^E$	$V_{m,chem}^E$	
BA + DMA	−0.192	−0.208	−0.177	−0.031	[24]
HxA + DMA	0.006	0.006	0.043	−0.036	[24]
DPA + DMA	−0.227	−0.232	−0.242	0.01	[24]
DBA + DMA	0.056	0.051	0.116	−0.065	[24]
BA + DMF	−0.263	−0.270	−0.132	−0.139	[23]
HxA + DMA	−0.021	−0.024	0.075	−0.099	[23]
DPA + DMF	−0.289	−0.291	−0.181	−0.110	[23]
DBA + DMF	0.018	0.015	0.126	−0.111	[23]
Aniline + DMA	−0.609[c]	−0.634	0.264	−0.898	[45]
Aniline + DMF	−0.662	−0.662	0.241	−0.903	[27]
	−0.693				[79]

[a]For symbols, see Table 1; [b]results using ERAS parameters from Table 5; [c]T = 303.15 K; X_{AB} = 5 J·cm^{-3}.

Table 7

Excess functions, permittivity, ε_r^E, orientational polarizability, $(\Pi_m^{or})^E$, and relative Kirkwood's correlation factors ($g_{K,rel}^E$, $g_{K,rel,i}^E$, i = 1,2) for *N,N*-dialkylamide (1) + amine (2) mixtures at ϕ_1 = 0.5 and 298.15 K. The minimum and maximum values of ε_r^E, $g_{K,rel}^E$, $g_{K,rel,i}^E$ (i = 1,2) and the corresponding compositions are also listed.

System[a]	ε_r^E	$(\Pi_m^{or})^E$ / $cm^3 \cdot mol^{-1}$	$g_{K,rel}^E$	$g_{K,rel,1}^E$	$g_{K,rel,2}^E$
		$\phi_1 = 0.5$			
DMA + BA	−1.943	−42.6	−0.10	−0.10	−0.10
DMA + HxA	−2.305	−56.4	−0.12	−0.12	−0.12
DMA + DPA	−2.348	−59.2	−0.12	−0.12	−0.12
DMA + DBA	−2.586	−69.5	−0.13	−0.13	−0.13
DMF + BA	−0.864	−18.0	−0.05	−0.05	−0.05
DMF + HxA	−1.262	−27.8	−0.07	−0.07	−0.06
DMF + DPA	−1.372	−31.6	−0.08	−0.08	−0.08
DMF + DBA	−1.733	−41.4	−0.09	−0.09	−0.09
DMF + aniline	1.806	30.5	0.10	0.08	0.08

	Minimum or maximum values							
	ϕ_1	ε_r^E	ϕ_1	$g_{K,rel}^E$	ϕ_1	$g_{K,rel1}^E$	ϕ_1	$g_{K,rel2}^E$
DMA + BA	0.45	−1.98	0.19	−0.14	0.17	−0.15	0.18	−0.14
DMA + HxA	0.46	−2.32	0.20	−0.18	0.15	−0.19	0.15	−0.18
DMA + DPA	0.43	−2.39	0.17	−0.21	0.11	−0.22	0.12	−0.21
DMA + DBA	0.45	−2.62	0.18	−0.24	0.10	−0.24	0.11	−0.24
DMF + BA	0.35	−0.97	0.20	−0.09	0.15	−0.09	0.15	−0.09
DMF + HxA	0.36	−1.38	0.22	−0.13	0.14	−0.13	0.14	−0.13
DMF + DPA	0.37	−1.51	0.22	−0.15	0.12	−0.16	0.14	−0.15
DMF + DBA	0.38	−1.86	0.26	−0.18	0.14	−0.18	0.14	−0.18
DMF + aniline	0.39	1.976	0.25	0.12	0.28	0.11	0.25	0.13

[a]For symbols, see Table 1

Table 8

Values of $V_m \frac{\partial \varepsilon_r^*}{\partial T}$/cm^3·mol^{-1}·K^{-1} at 298.15 K for *N,N*-dialkylamide (1) + amine (2) mixtures at 298.15 K and ϕ_1=0.5

Amide	BA	HxA	DPA	DBA	Aniline
DMA	–9.86	–10.9	–11.1	–11.6	
DMF	–8.27	–8.80	–8.90	–8.81	–9.31

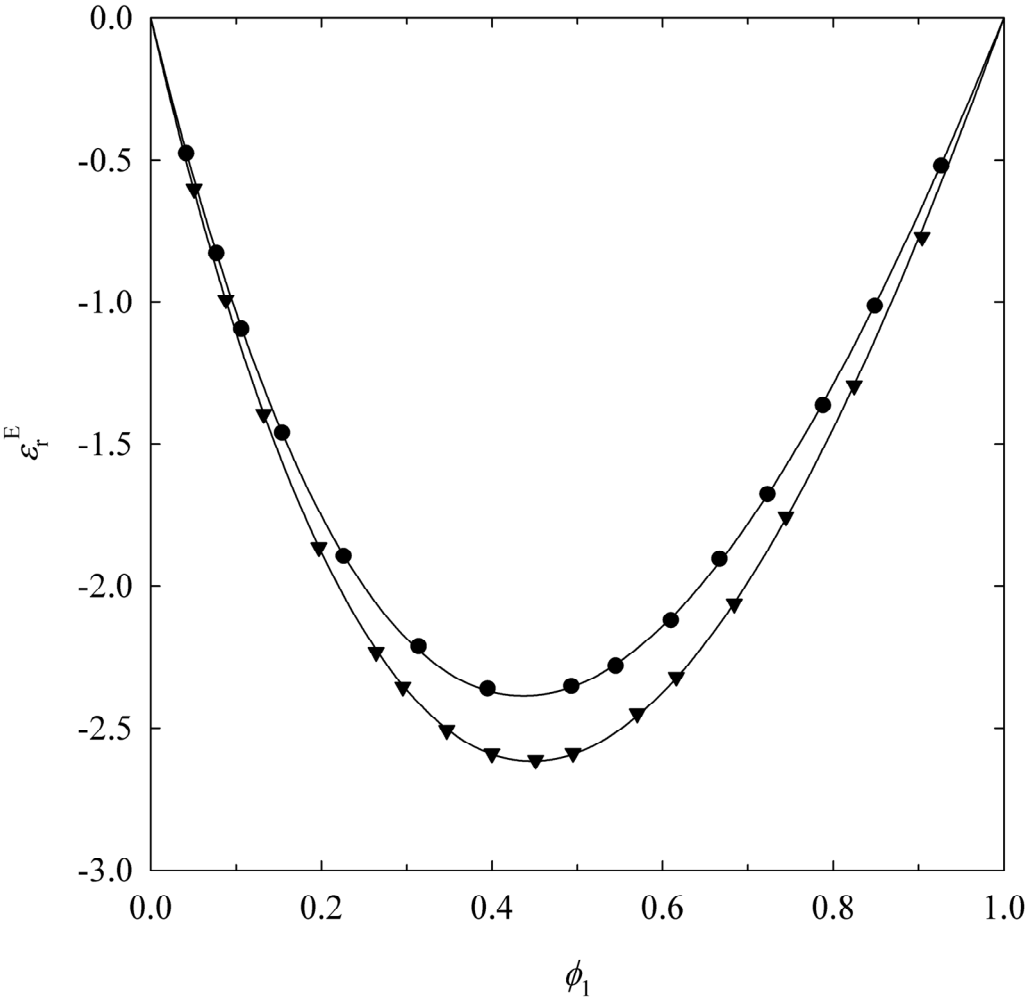

Figure 1

Excess relative permittivities, ε_r^E, for DMA (1) + DPA (2), or + DBA (2) systems at 0.1 MPa, 298.15 K and 1 MHz. Full symbols, experimental values (this work): (●), DPA; (▼), DBA. Solid lines, calculations with equation (3) using the coefficients from Table 4.

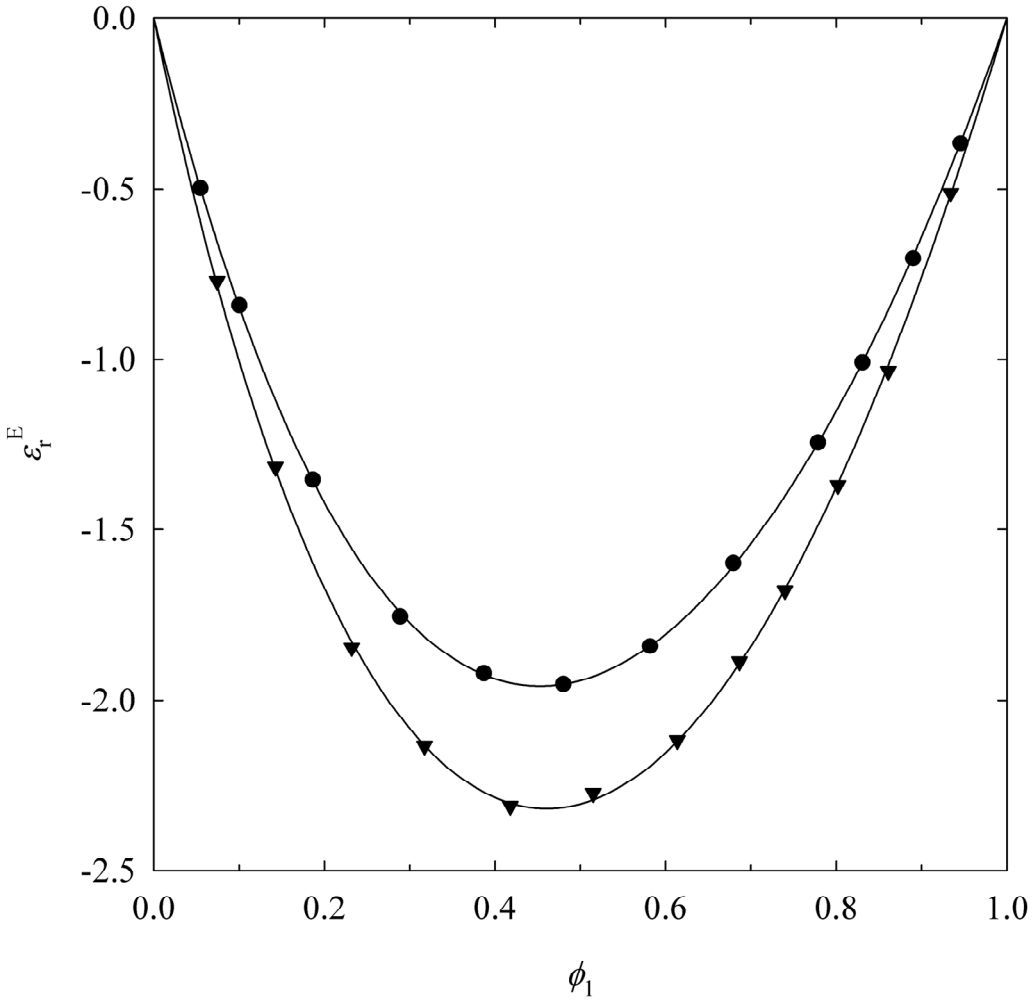

Figure 2

Excess relative permittivities, ε_r^E, for DMA (1) + BA (2), or + HxA (2) systems at 0.1 MPa, 298.15 K and 1 MHz. Full symbols, experimental values (this work): (●), BA; (▼), HxA. Solid lines, calculations with equation (3) using the coefficients from Table 4.

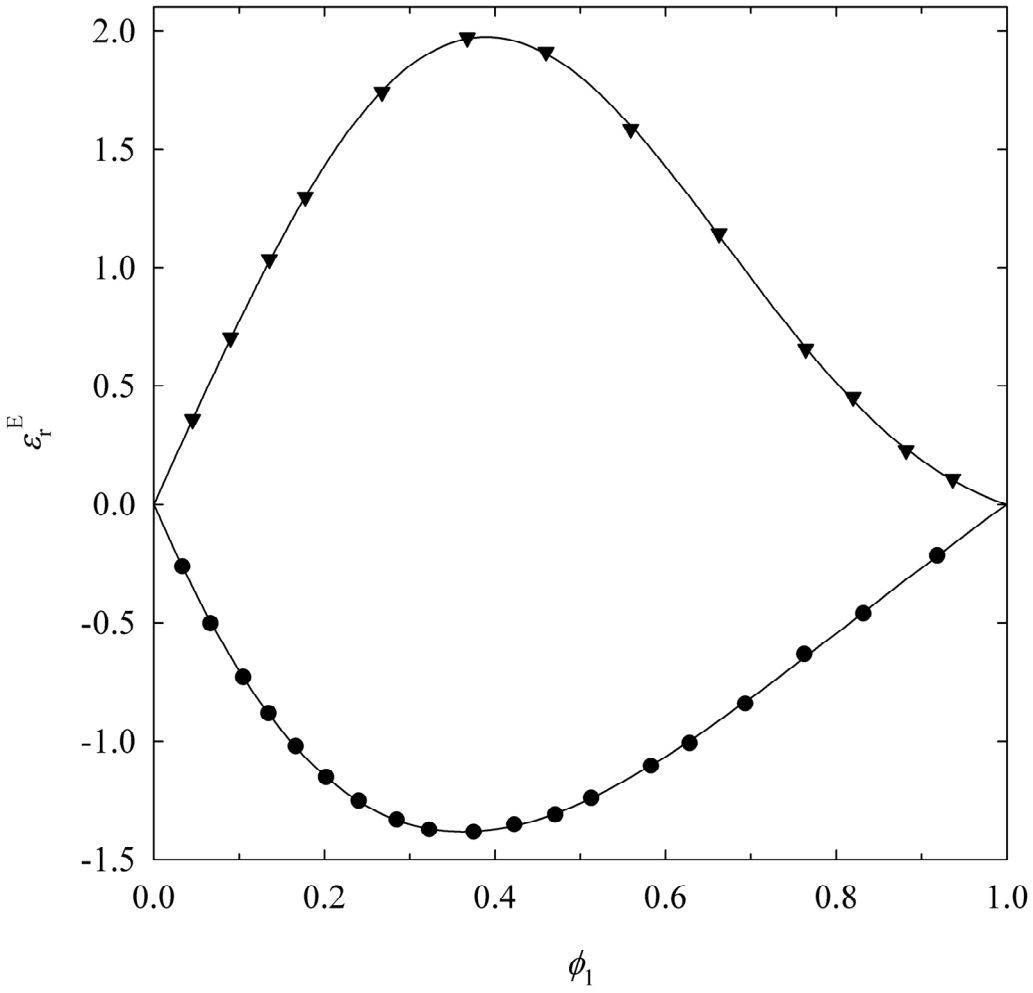

Figure 3

Excess relative permittivities, ε_r^E, for DMF (1) + amine (2) systems at 0.1 MPa, 298.15 K and 1 MHz. Full symbols, experimental values: (▼), aniline (this work); (●), HxA [25]. Solid lines, calculations with equation (3) using the coefficients from Table 4 or from the literature [25].

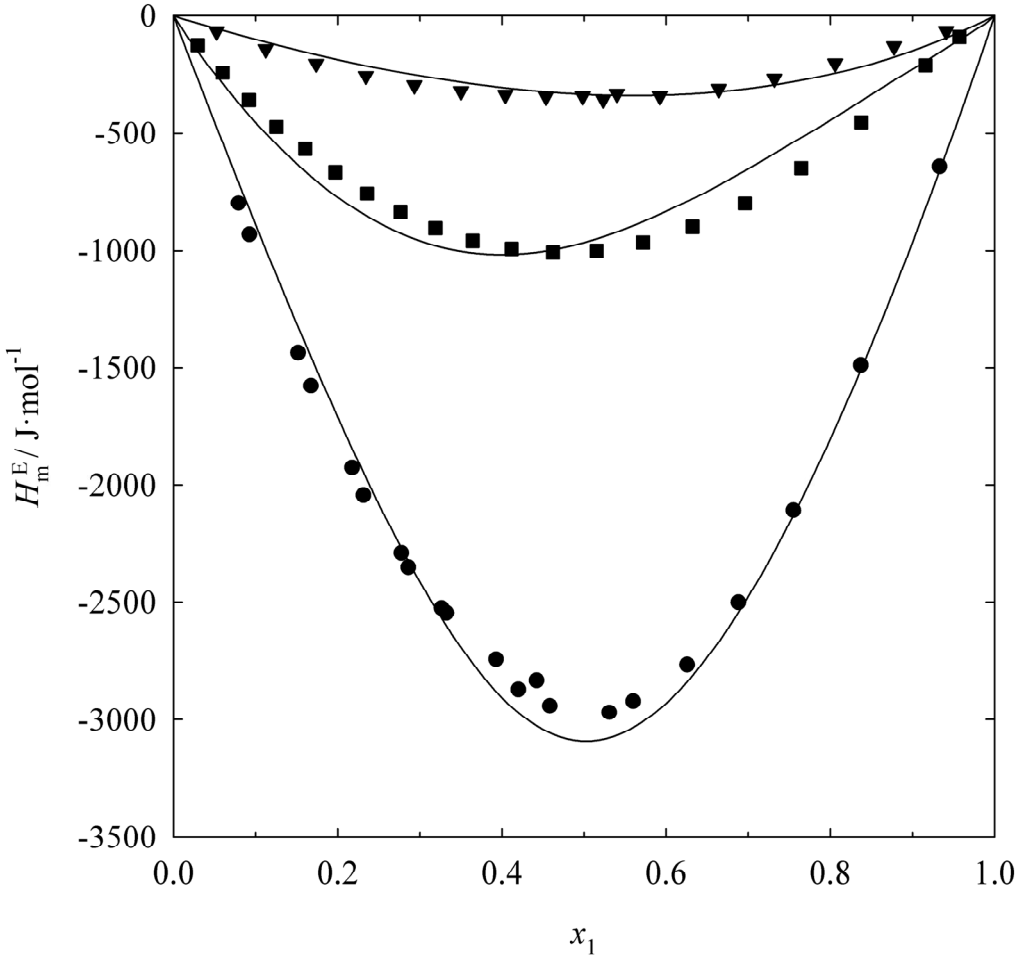

Figure 4

Excess molar enthalpies, H_m^E for amine (1) + amide (2) mixtures at 0.1 MPa. Points experimental results: (●), aniline (1) + DMF (2) (T = 298.15 K) [18]; (■), HxA (1) + NMA (2) (T =363.15 K) [20]; (▲), aniline (1) + DMA (2) (T = 298.15 K) [19]. Solid lines, ERAS calculations with parameters from Table 5.

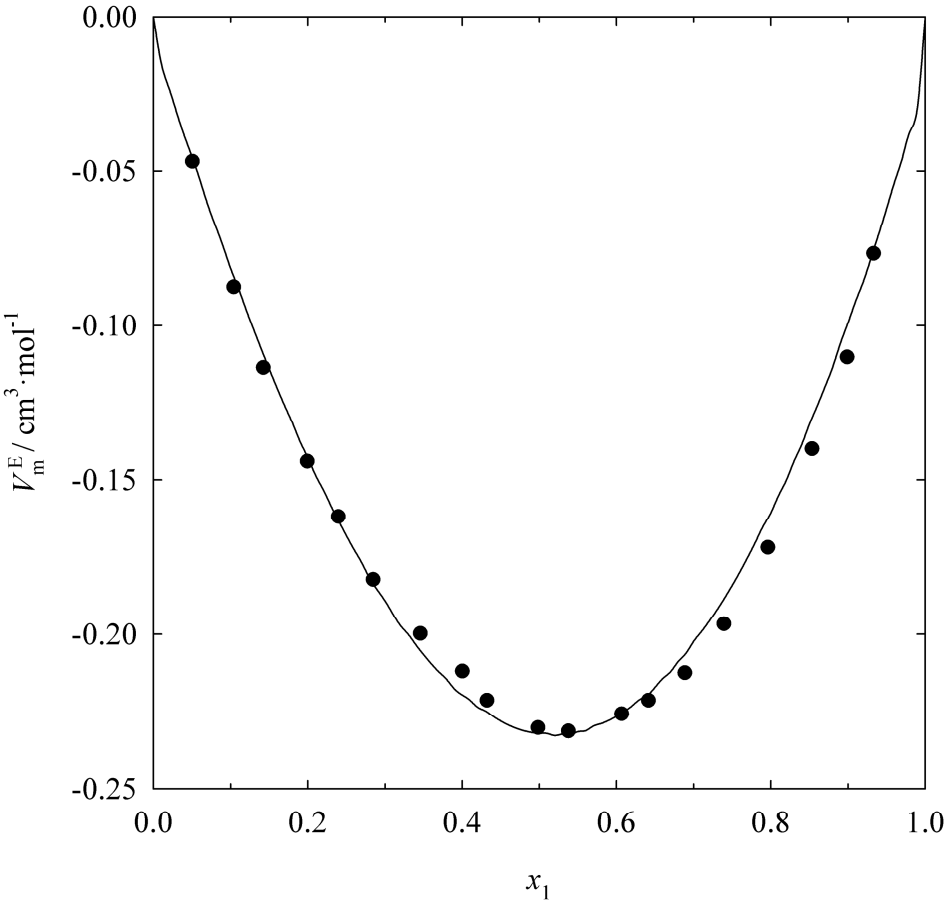

Figure 5

Excess molar volume, V_m^E for DPA (1) + DMA (2) mixture at 298.15 K and 0.1 MPa. Points experimental results [24]. Solid line, ERAS calculations with parameters from Table 5.

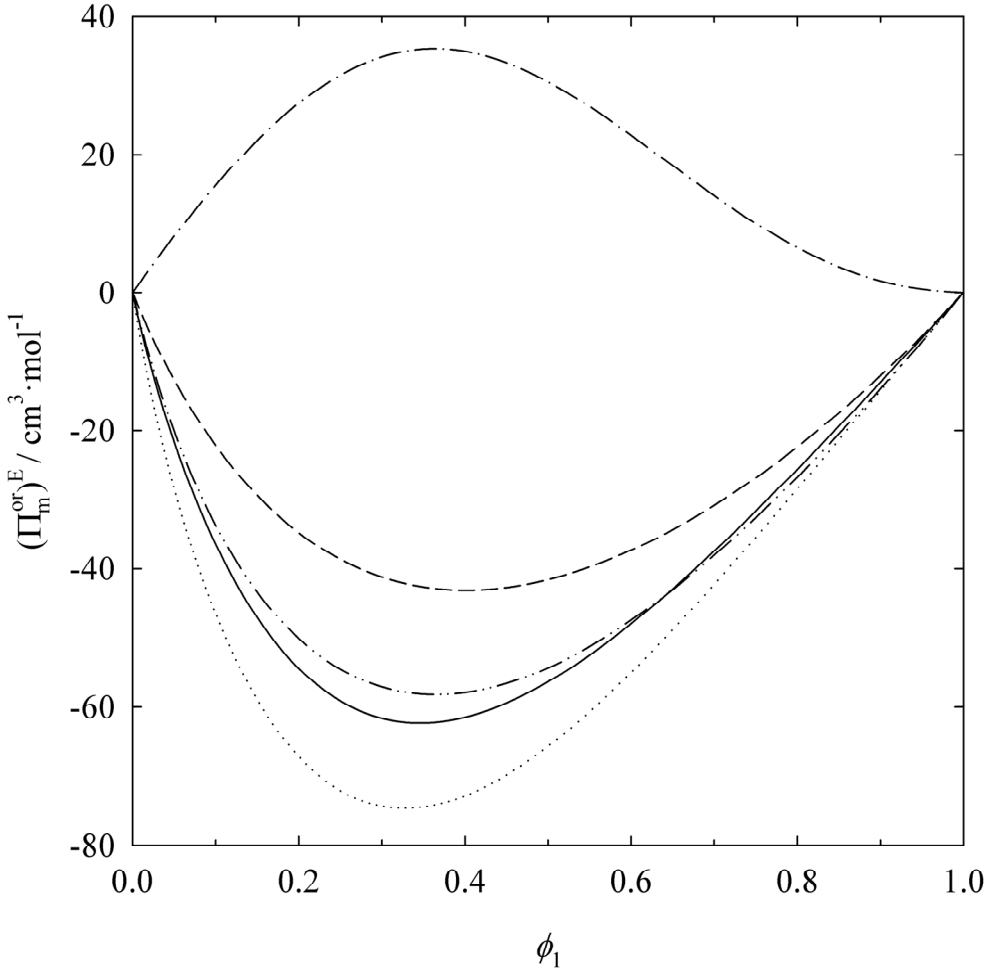

Figure 6

Excess molar orientational polarizability, $(\Pi_m^{or})^E$, for DMA (1) + linear amine (2), or DMF (1) + aniline (2) systems at 0.1 MPa and 298.15 K. (——), DMA + DPA; (···), DMA + DBA; (– – –), DMA + BA; (··–··), DMA + HxA; (·–·), DMF + aniline.

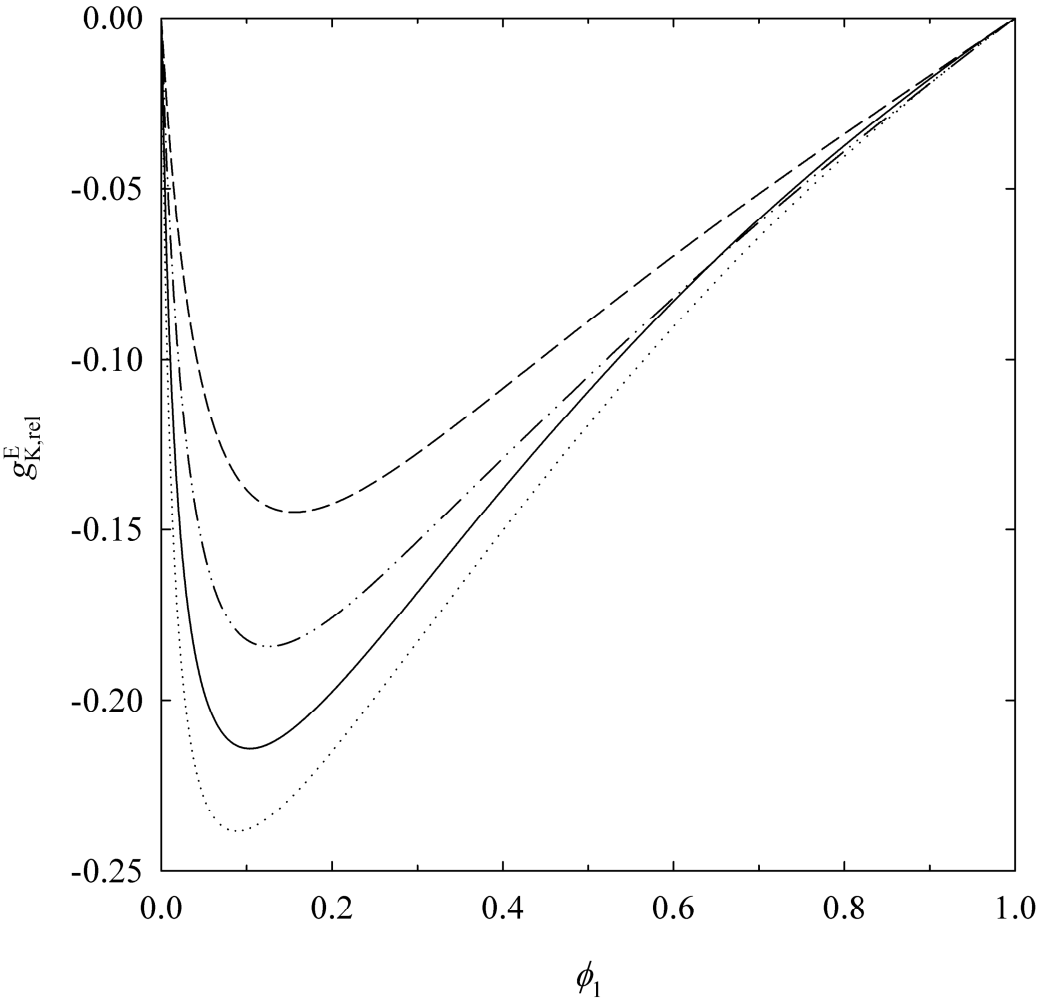

Figure 7

Excess relative Kirkwood correlation factors, $g^{E}_{K,rel}$, of DMA (1) + amine (2) systems at 0.1 MPa and 298.15 K. (——), DMA + DPA; (···), DMA + DBA; (– – –), DMA + BA; (··–··), DMA + HxA.

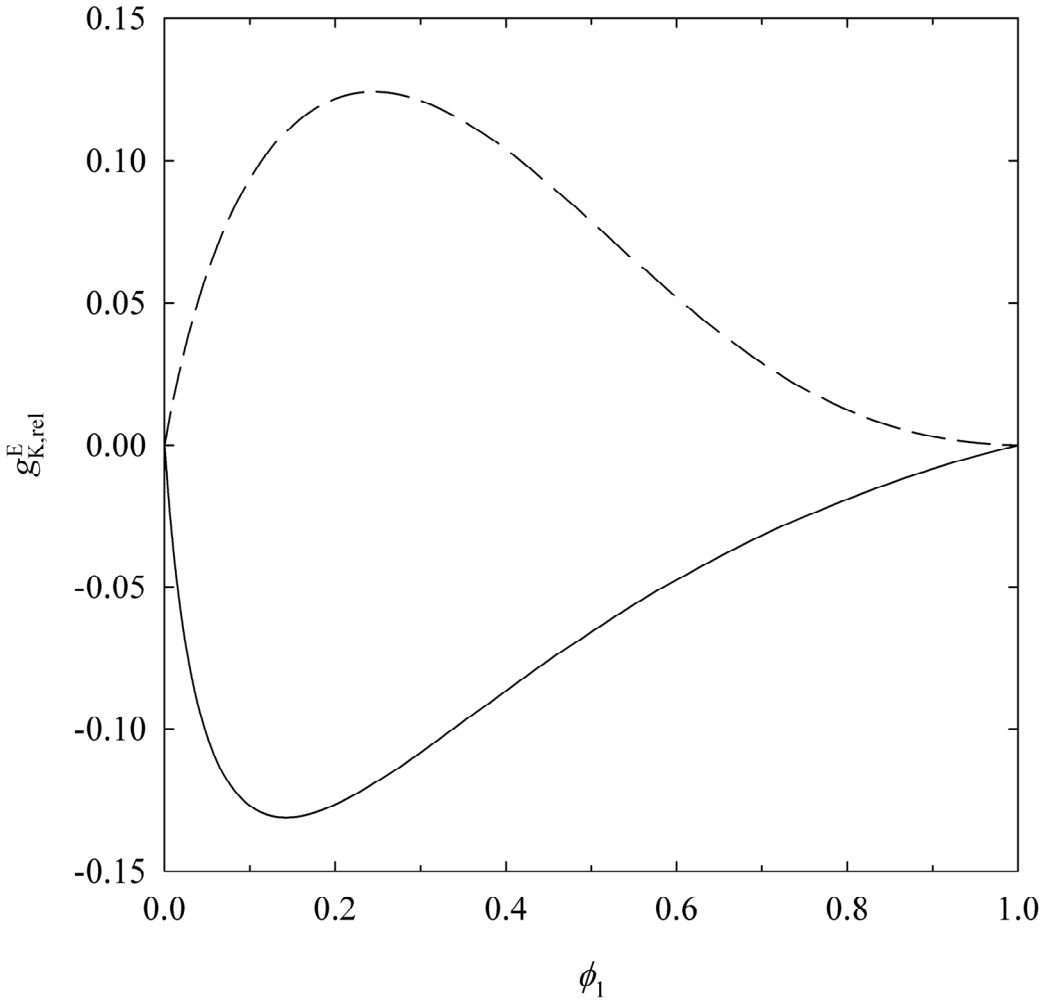

Figure 8

Excess relative Kirkwood correlation factors, $g^{E}_{K,rel}$, of DMF (1) + amine (2) systems at 0.1 MPa and 298.15 K. (——), HxA [25]; (– – –), aniline (this work).

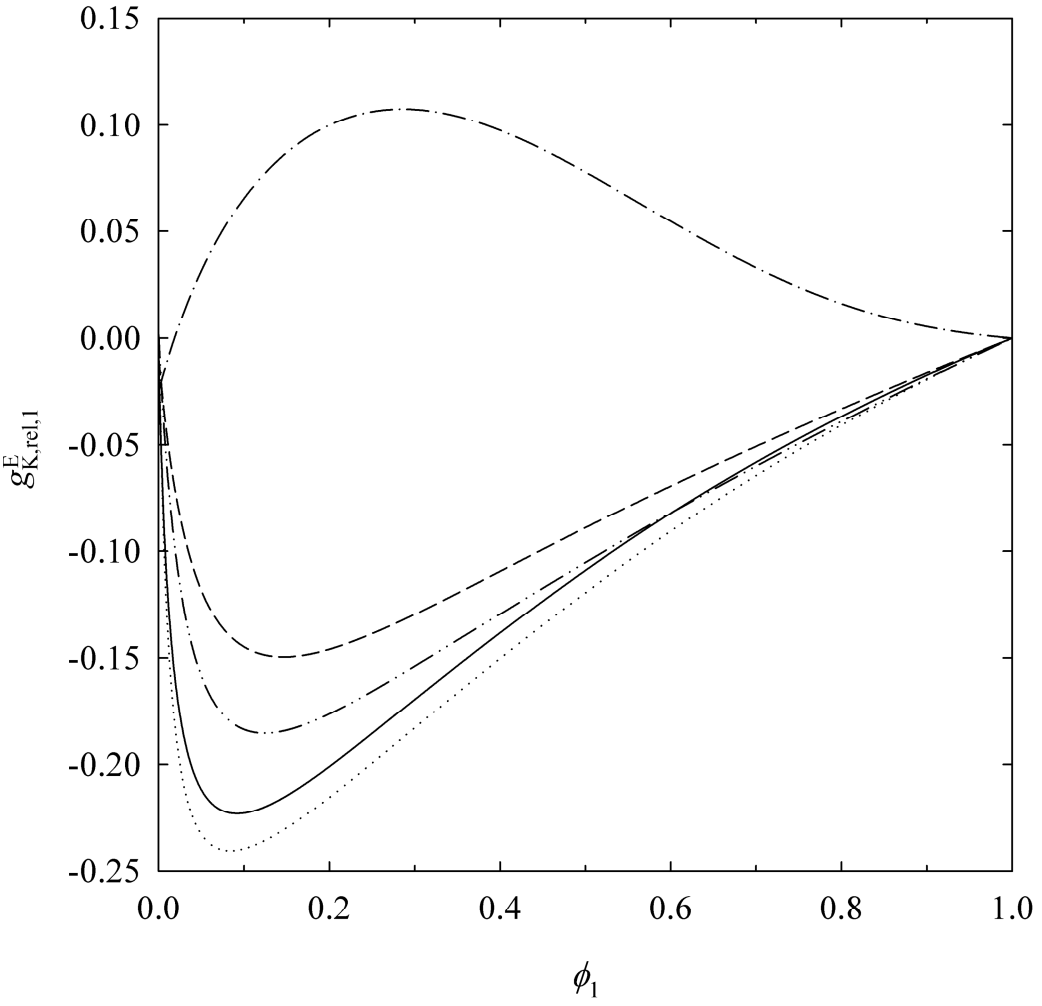

Figure 9

Excess relative Kirkwood correlation factors of liquid 1, $g^{E}_{K,rel,1}$, for DMA (1) + linear amine (2), or DMF (1) + aniline (2) systems at 0.1 MPa and 298.15 K. (– —), DMA + DPA; (···), DMA + DBA; (– – –), DMA + BA; (··–··), DMA + HxA; (·–·), DMF + aniline.

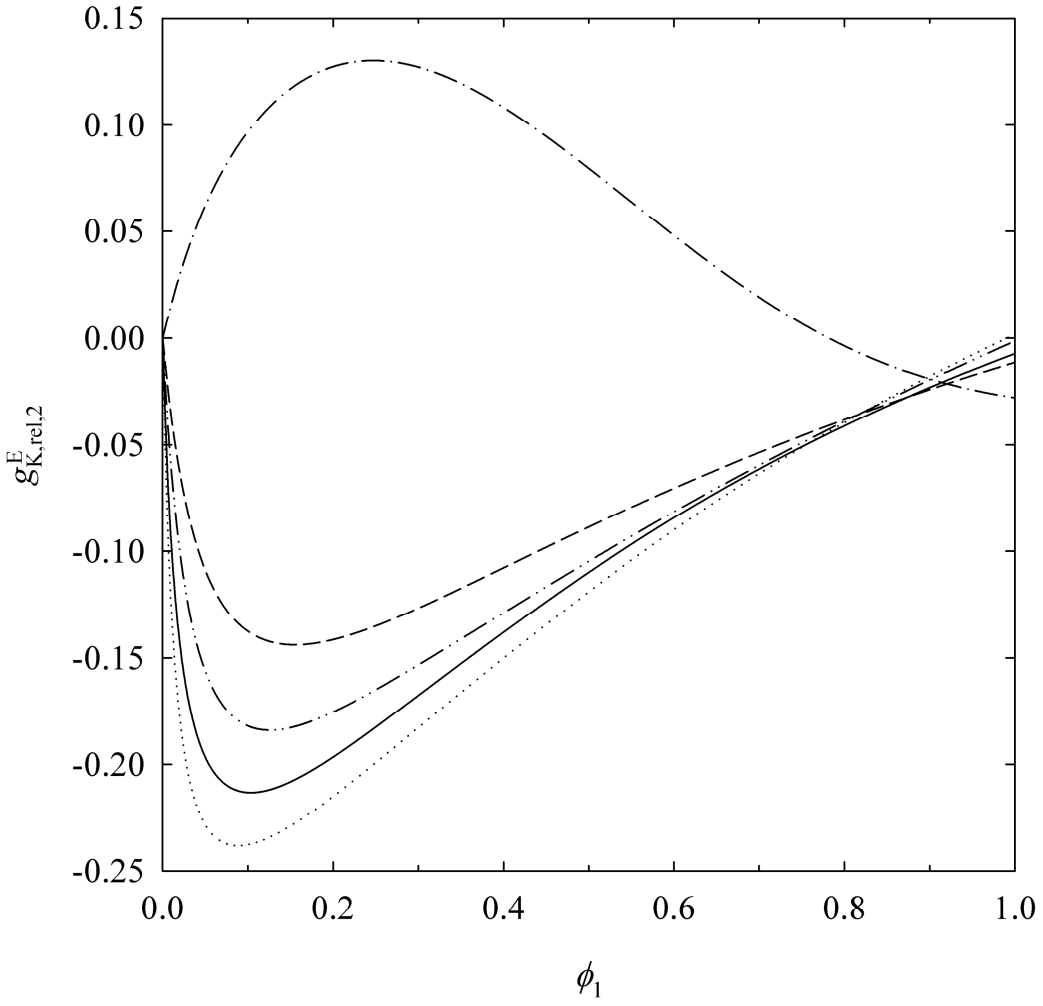

Figure 10

Excess relative Kirkwood correlation factors of liquid 2, $g^{E}_{K,rel,2}$, for DMA (1) + linear amine (2), or DMF (1) + aniline (2) systems at 0.1 MPa and 298.15 K. (– —), DMA + DPA; (···), DMA + DBA; (– – –), DMA + BA; (··–··), DMA + HxA; (·–·), DMF + aniline.

➡ ε_r and ε_r^E data at (293.15-303.15) K are given for DMA+BA, +HxA, +DPA, or +DBA and for DMF + aniline

➡ ε_r^E values are large and negative for linear amine mixtures and positive for the aniline solution

➡Longer linear amines are better breakers of the amide-amide interactions

➡Amide-amine interactions are more easily formed if shorter linear amines, or DMF, participate

➡Mixtures have been studied using the Kirkwood-Fröhlich and ERAS models

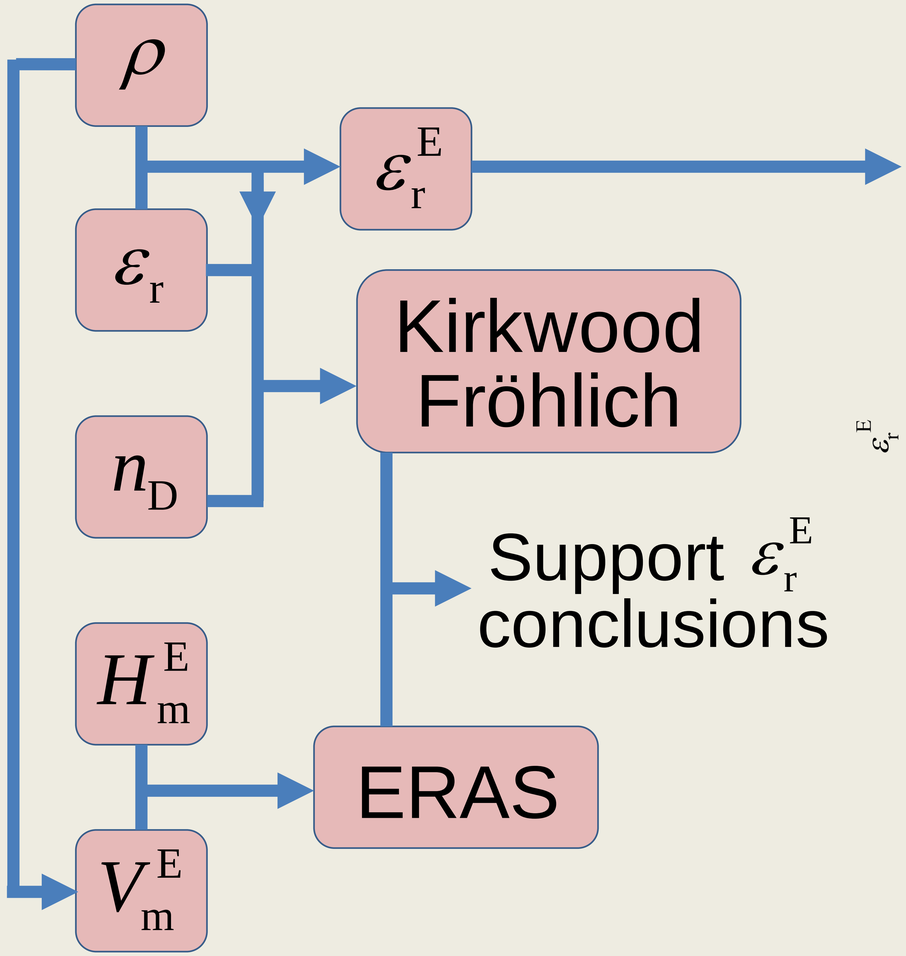

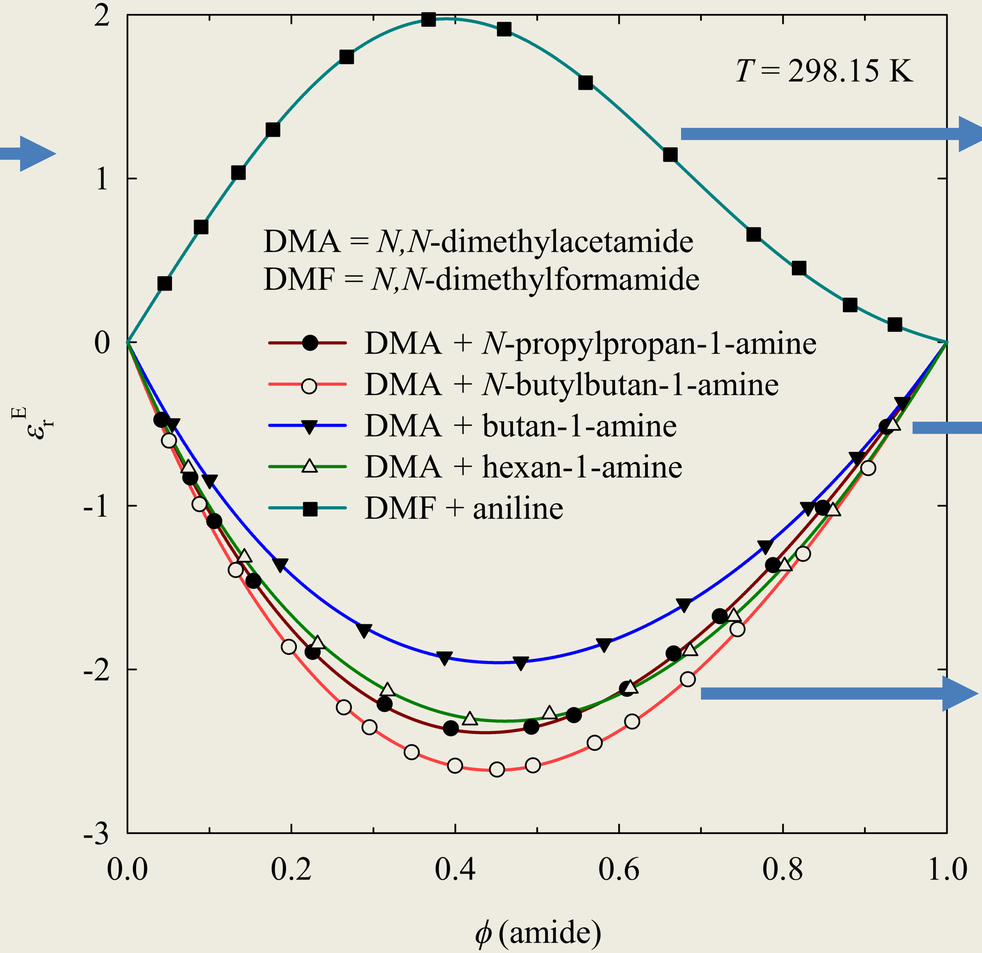

Strong DMF-aniline interactions

Dominant rupture of interactions

More effective amide-amide interaction breaking by longer amines